RICE

Bioengineering

Nanomedicine and Genome Editing Approaches for Disease Therapies

Gang Bao
Department of Bioengineering
Rice University
Houston, TX 77030

Funding: Cancer Prevention and Research Institute of Texas (RP220518)
NIH/NHLBI, Cure Sickle Cell Initiative (OT2HL154977)
NIH/NHLBI R01 (R01HL152314)
NIH/NHGRI R01 (R01HG011459)

Outline

- Magnetic nanoparticle heating
- Magnetic nanoclusters for treating cancer
- CRISPR/Cas9 genome editing for curing SCD

Biomedical Applications of Iron Oxide Magnetic Nanoparticles (MNPs)

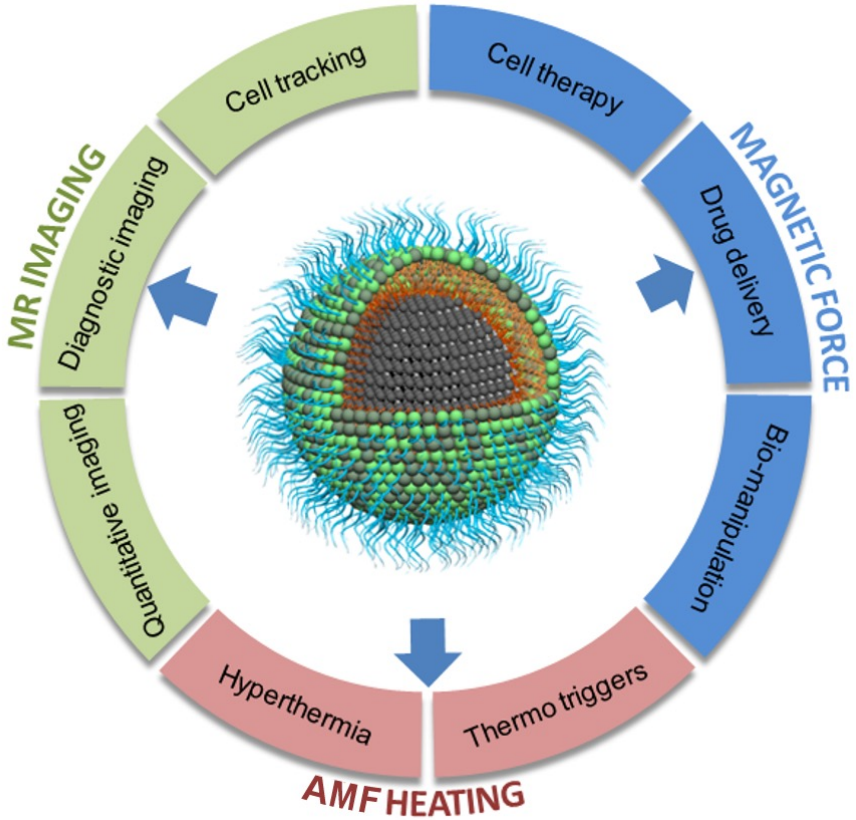

- **Iron oxide** NPs are non-toxic Fe_3O_4, γ-Fe_2O_3, $Fe_{1-x}O$
- The **phospholipid-PEG** coating is biocompatible
- Different core sizes, 6nm – 40nm
- Different coating thicknesses, PEG 750, 1000, 2000, 5000
- Stable coating, uniform size

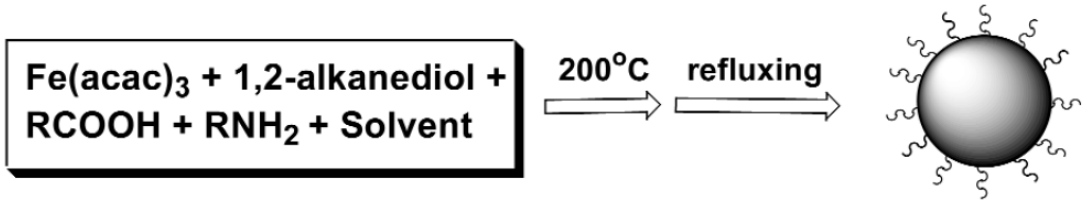

Magnetic Nanoparticle Heating

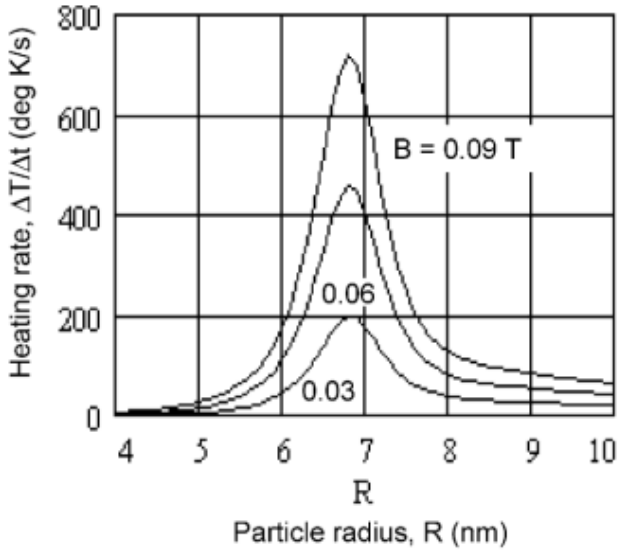

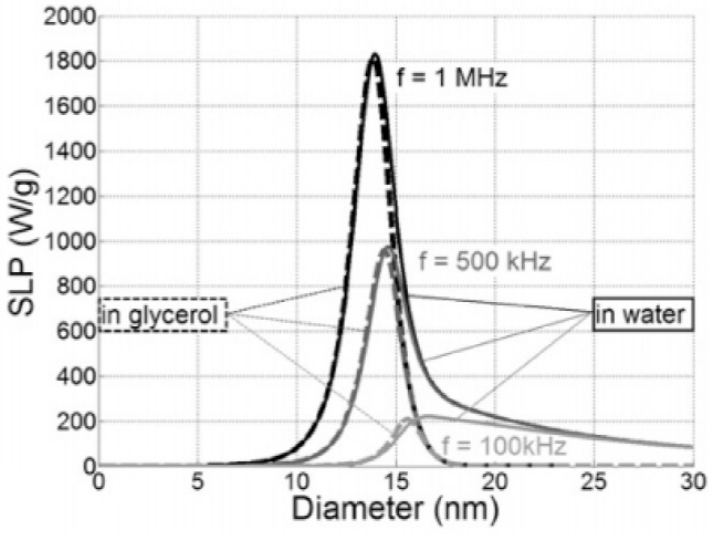

- Magnetic iron oxide nanoparticles (MNP) generate heat under an alternating magnetic field (AMF)
- The dependence of *specific absorption rate* (SAR) on MNP size has attracted extensive studies
- A theory developed in 2002 by R.E. Rosensweig (cited >2700 times) predicted that the peak of SAR occurs at ~14 nm, with large decrease of SAR below or above this critical size
- This theory is based on rotational relaxation of single-domain magnetic nanoparticles dispersed in a fluid

Rosensweig, R.E., 2002

RICE

Bioengineering

Iron Oxide Nanoparticles

Magnetite (Fe_3O_4) and Maghemite (γ-Fe_2O_3)

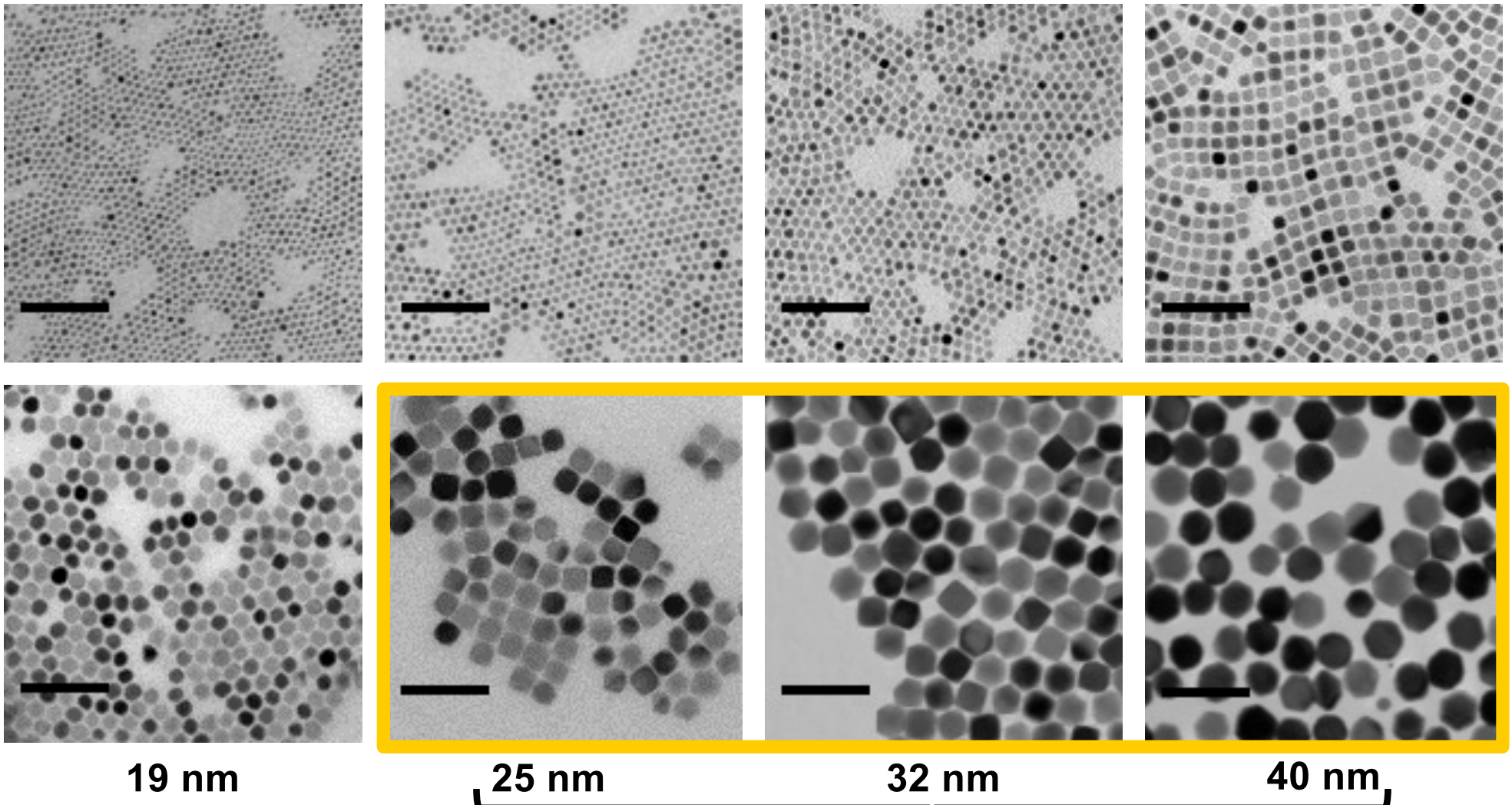

Scale bar = 100 nm

Above presumed superparamagnetic size limit

SAR Measurements

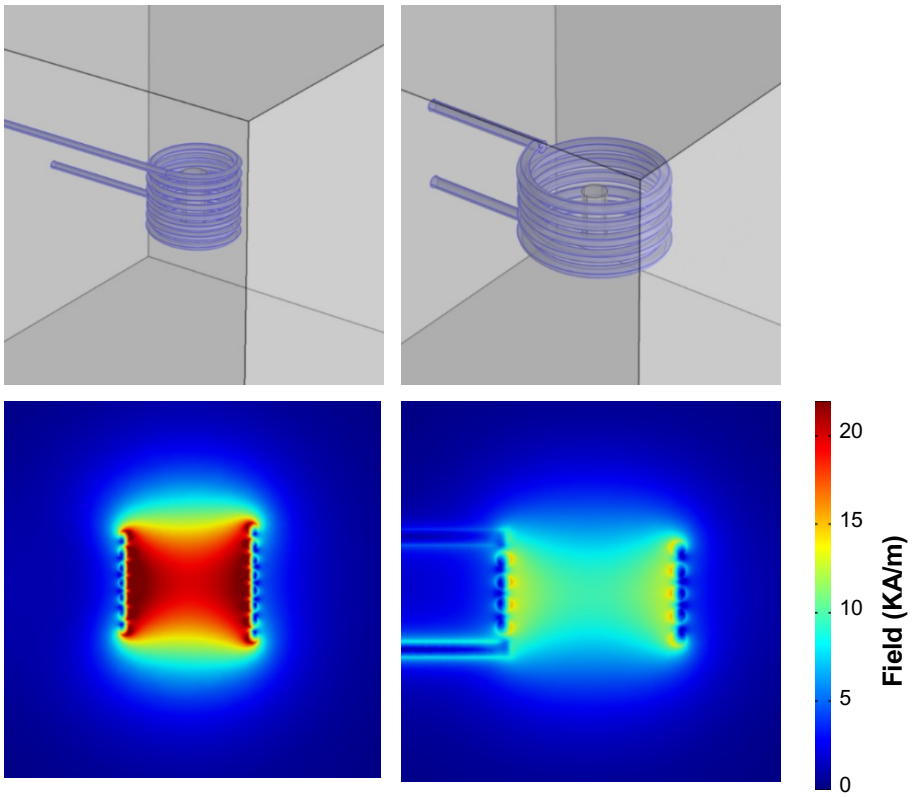

D = 2.5 cm, H = 3 cm
7.5 turns, I = 115 A

D = 5 cm, H = 3 cm
5 turns, I = 130 A

- For measuring SAR, MNPs dispersed in an aqueous solution were exposed to an alternating magnetic field generated with two different inductive coils at a fixed frequency (f = 325 kHz)
- The average field strength H applied to the solution was 9.35 kA/m or 20.7 kA/m
- The temperature of the ferrofluid was measured as a function of time and the slopes of the heating profiles were used to calculate the SAR values

Tong S *et al*, ACS Nano, 2017

Challenge to the Classical Theory

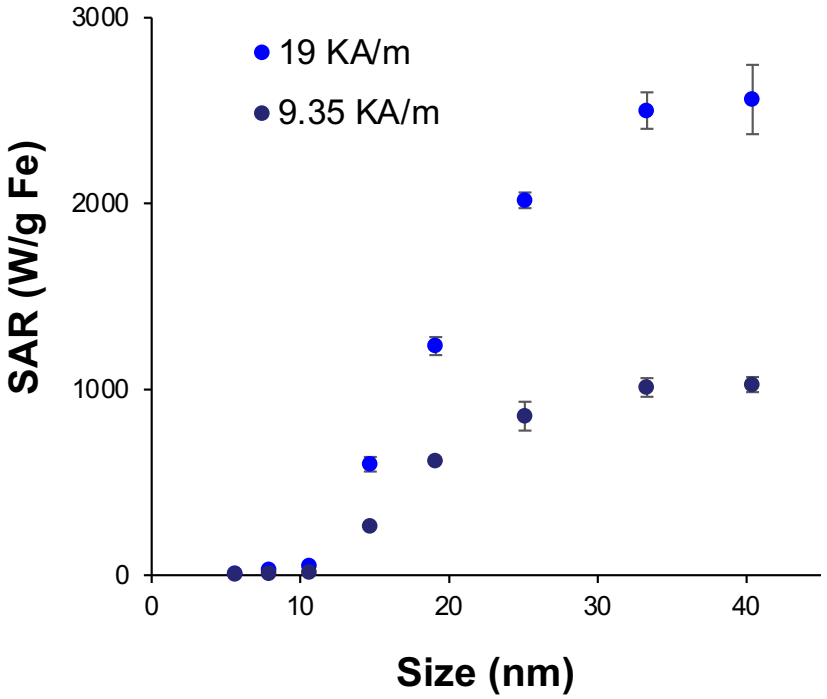

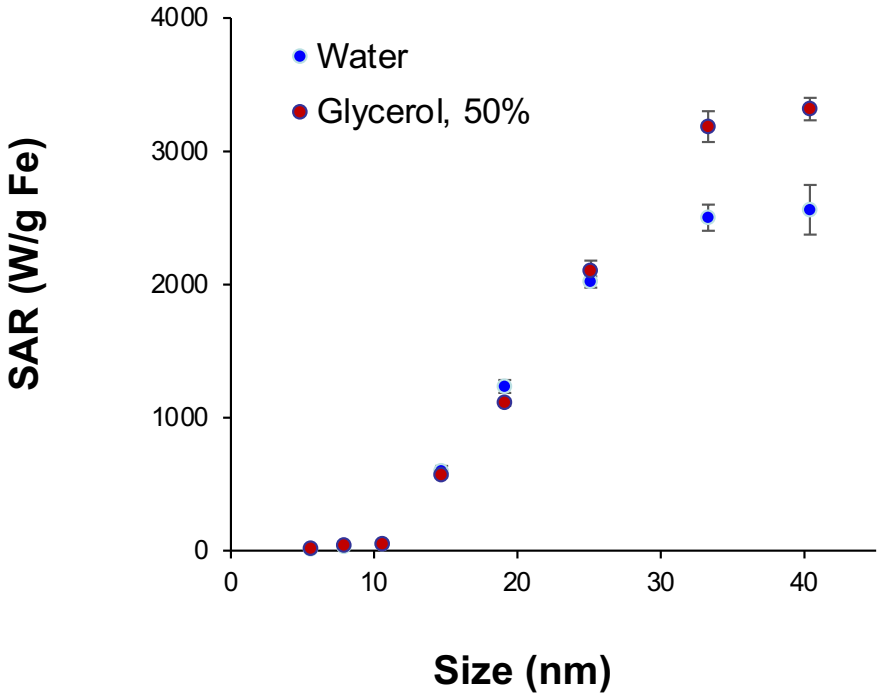

- The monotonic increase in SAR for MNPs < 40nm is in sharp contrast with the classical theory and some of the previous findings that SAR decreased when the size of MNPs becomes >15 nm
- **Independent measurements in the Bischop lab confirmed our results**

Tong S *et al*, ACS Nano, 2017

Micro-hysteresis Curves at 300K

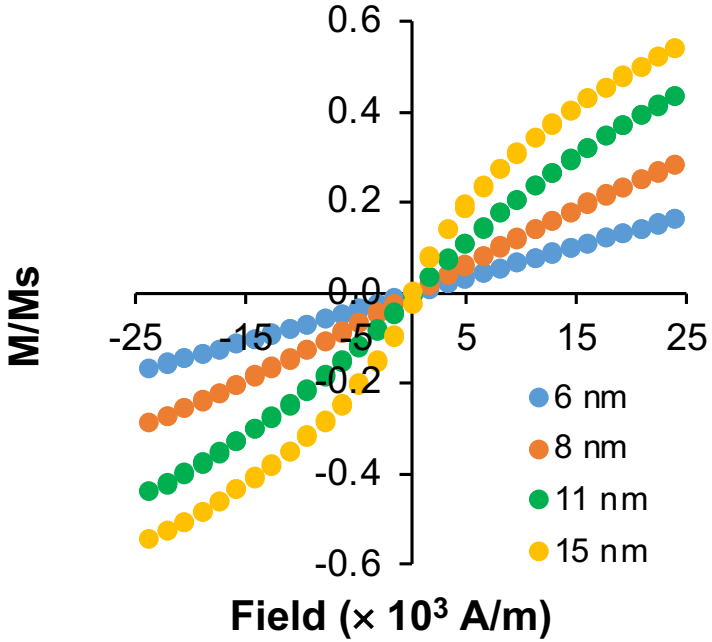

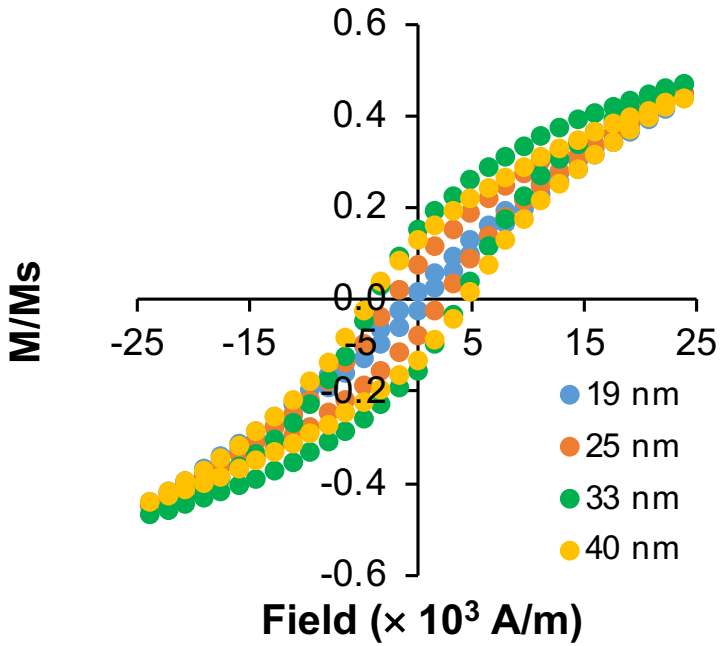

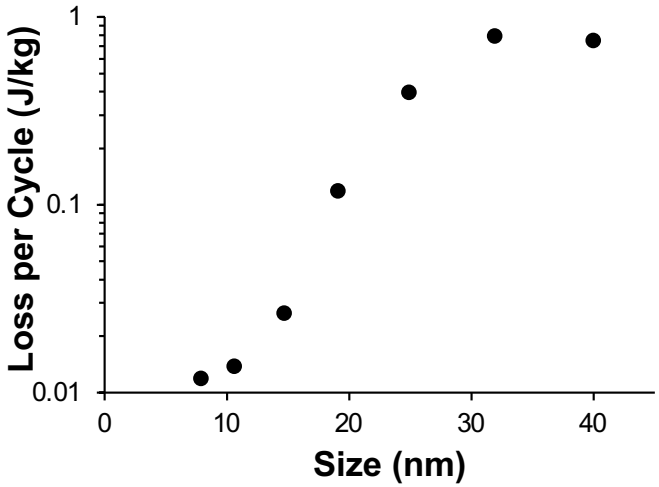

The classical linear response theory (LRT) assumes that

$$M(t) = \mathrm{Re}[\chi H_0 e^{i\omega t}]$$

which neglects hysteresis

Tong S *et al*, ACS Nano, 2017

Modified Dynamic Hysteresis Model

$$A = 3.53\mu_0 M_s H_{Max}(1 - 0.7\kappa)$$ **A: Heat generated by MNPs**

$$\kappa = \frac{K_B T}{K_A V} ln\left(\frac{K_B T}{4\mu_0 M_S V H f \tau_0}\right)$$, K_A anisotropy constant, M_s saturation magnetization
$\tau_0 = 1 \times 10^{-10}$ s, μ_0 magnetic permeability of vacuum

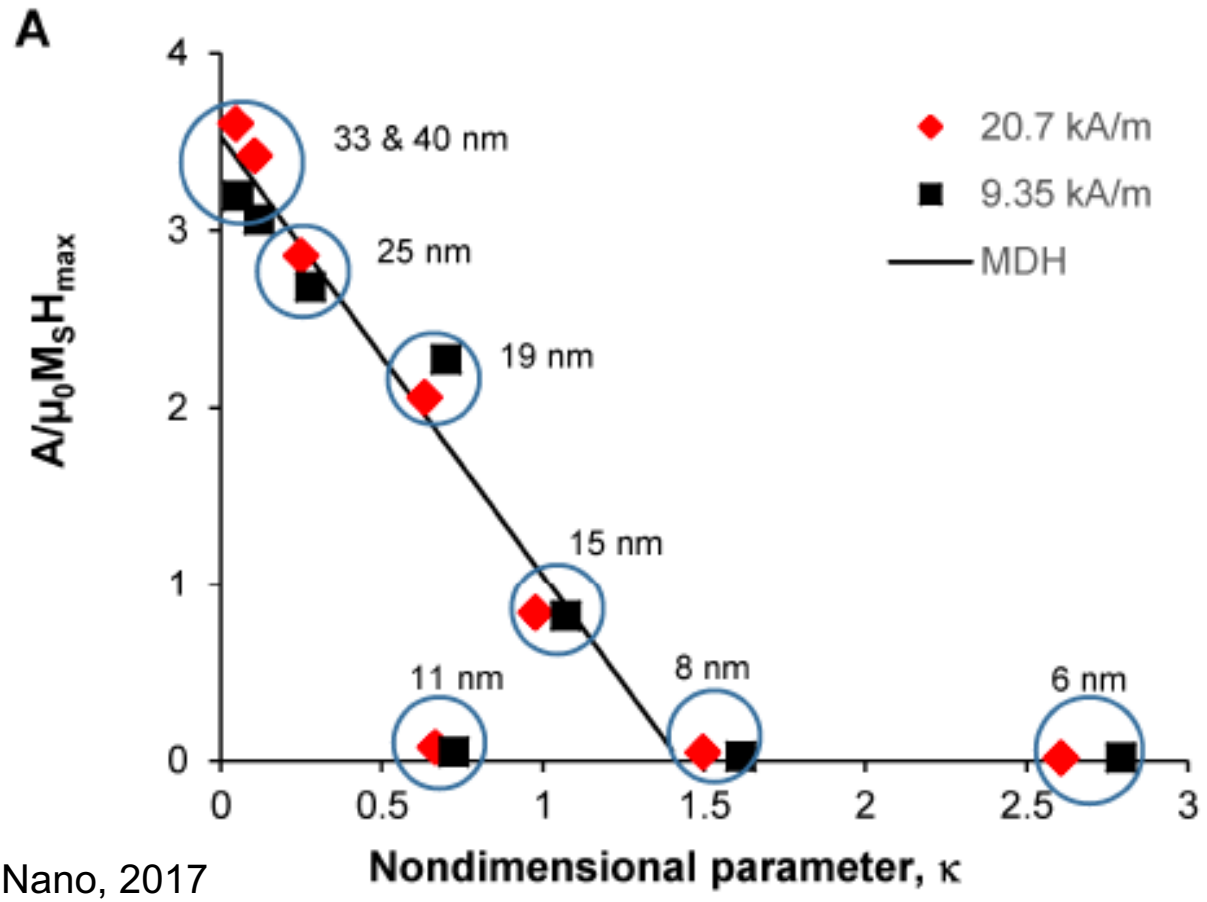

Tong S *et al*, ACS Nano, 2017

Our New Model Works Much Better

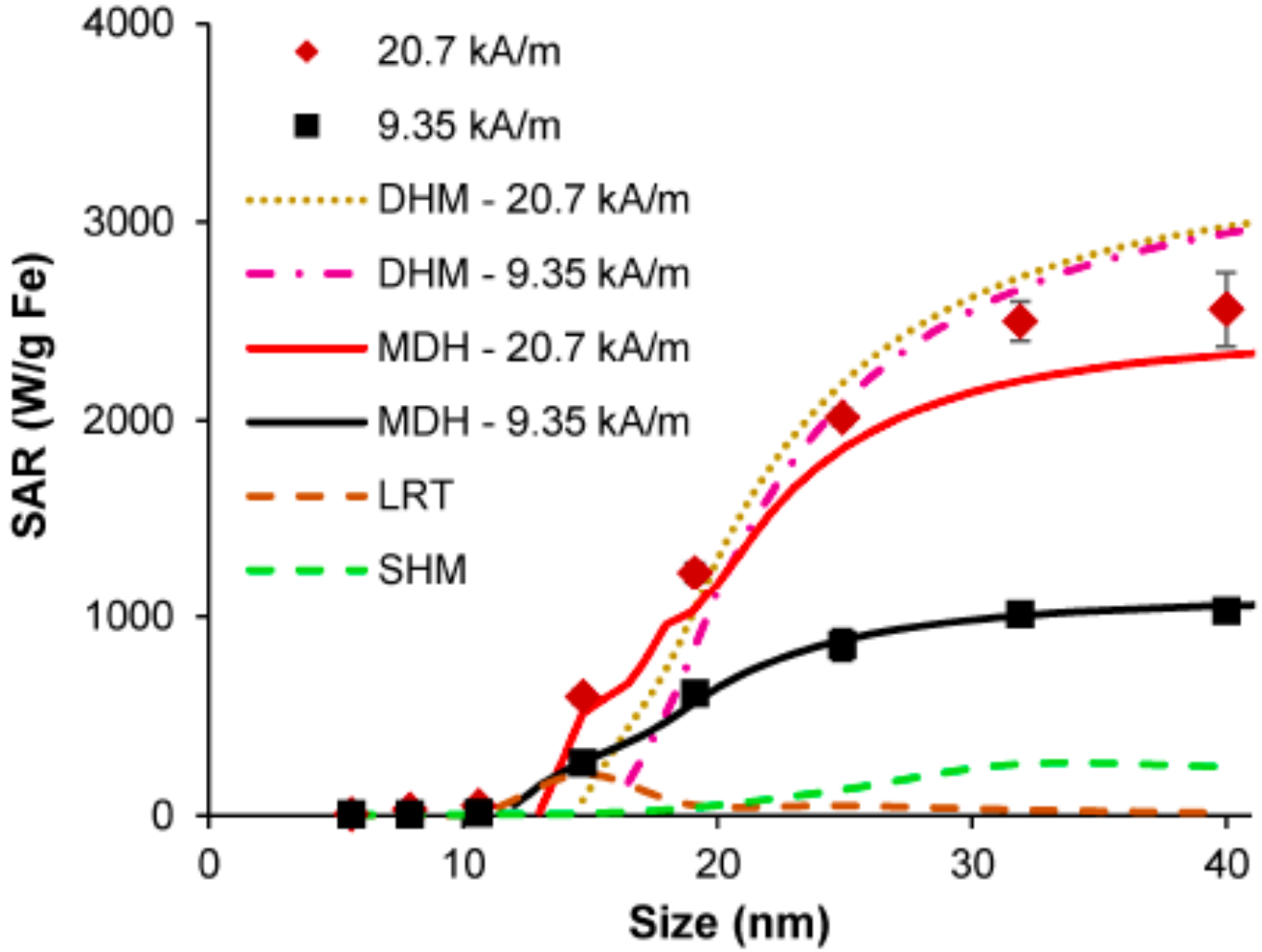

Tong S *et al*, ACS Nano, 2017

In Vivo Magnetic Nanoparticle Heating in Tumor Tissue

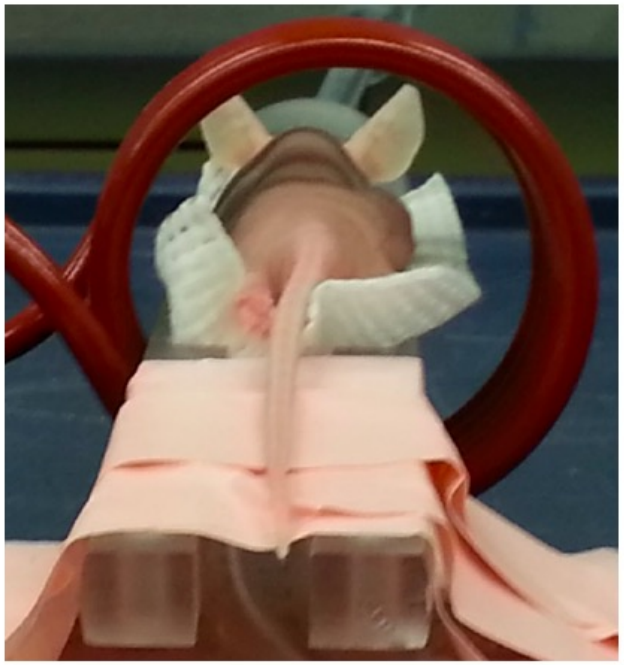

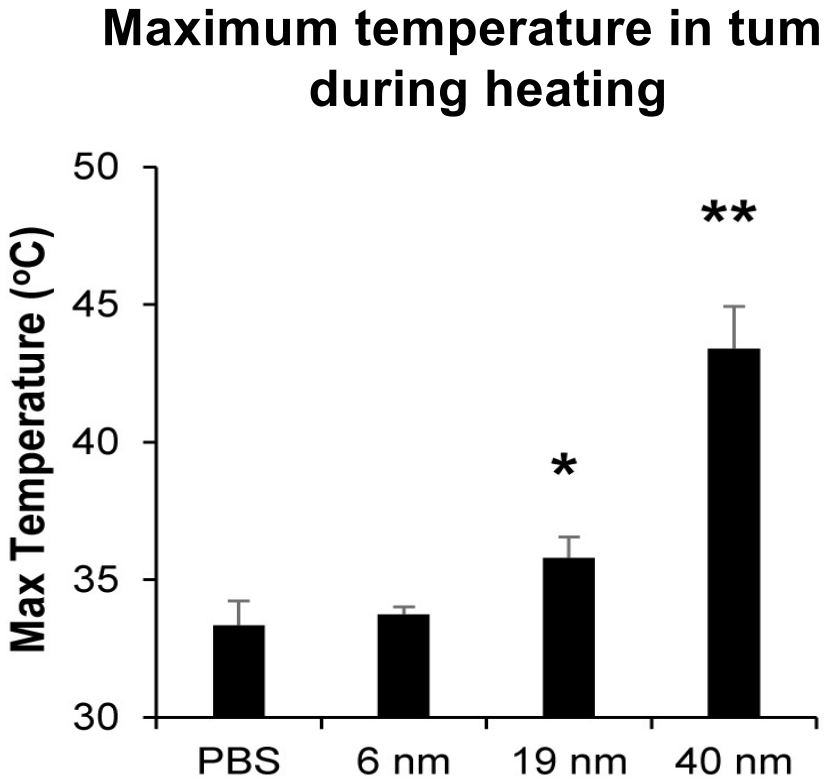

Solutions containing 50 μg of Fe/mL of MNPs were infused into the center of U87 tumors on the flank of mice. **Magnetic field was applied for 1 h** at 9.35 kA/m and 325 kHz. Note that the temperature of the tumor was lower than normal (~36.9° C) due to anesthesia.

Tong S *et al*, ACS Nano, 2017

RICE

Bioengineering

Magnetic Nanoclusters

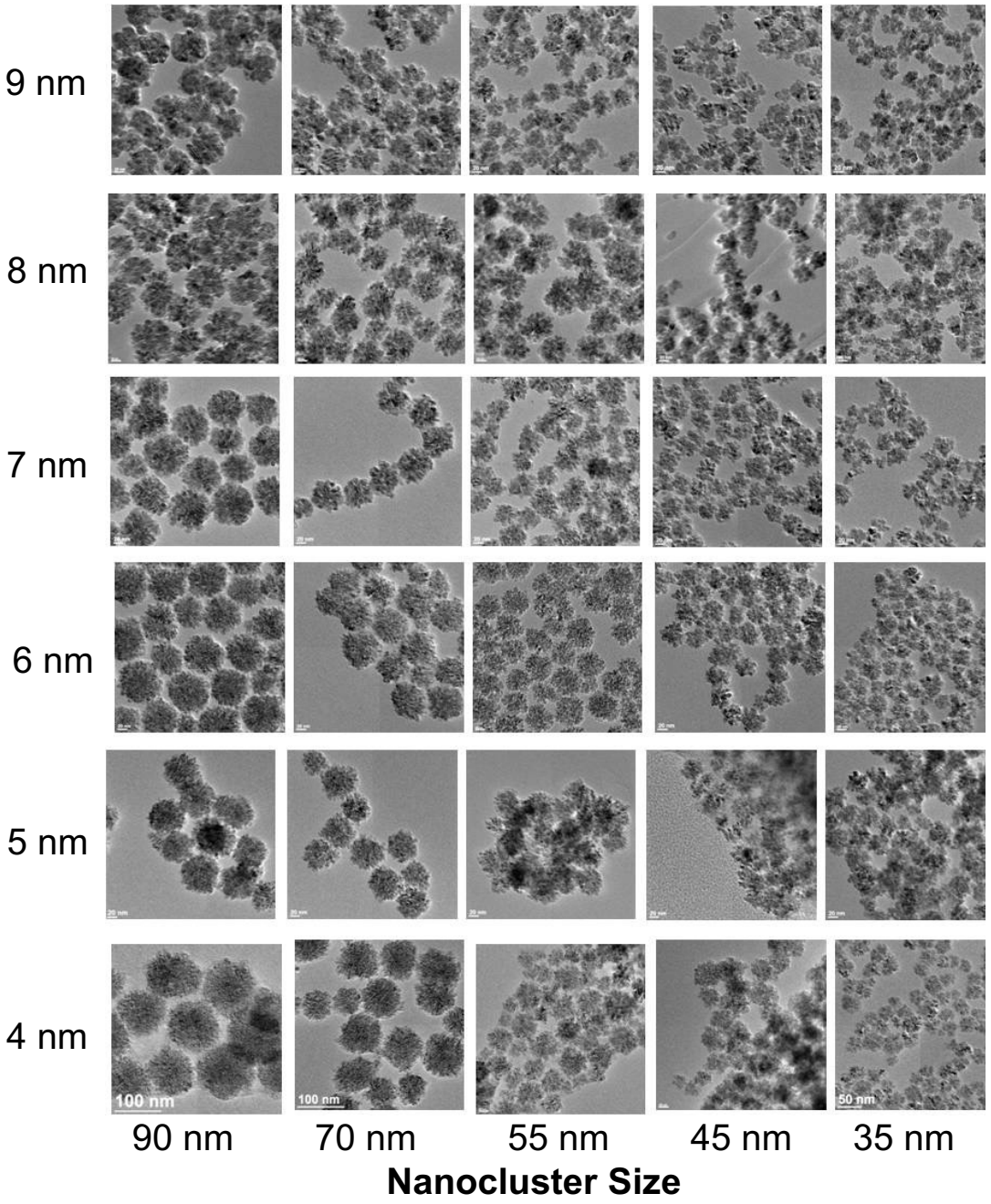

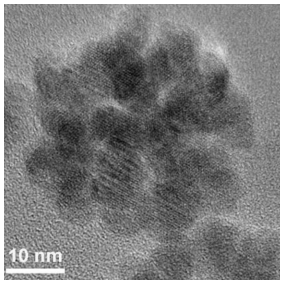

- Iron oxide nanoclusters (IONCs) composed of tens to hundreds of sub-10 nm iron oxide nanocrystals aggregated into larger, porous nanoclusters
- It's nano-size, in combination of superparamagnetism and large magnetic volume, offer unique properties such as high heat generation and MRI contrast
- The biomedical applications of IONCs have not been well explored

Magneto-thermotherapy

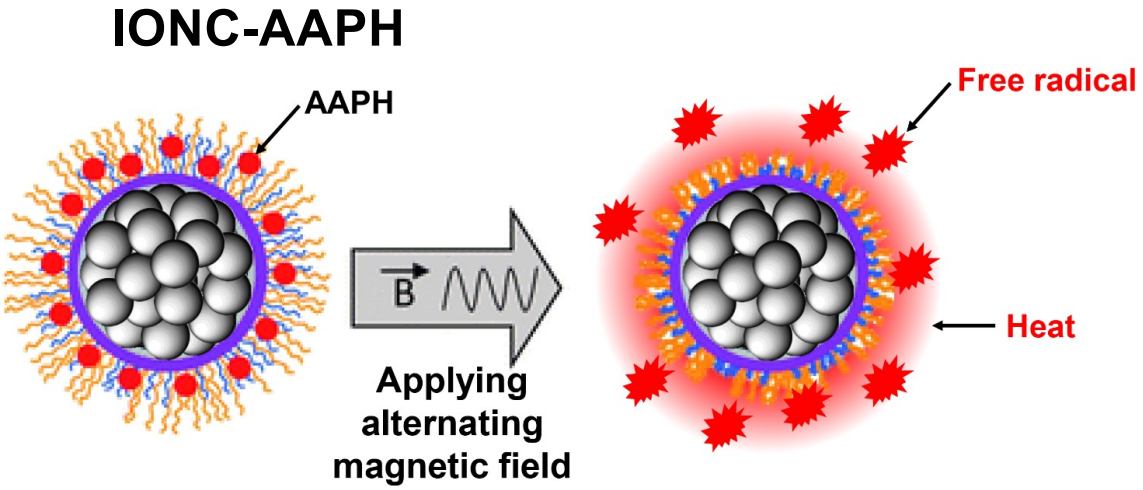

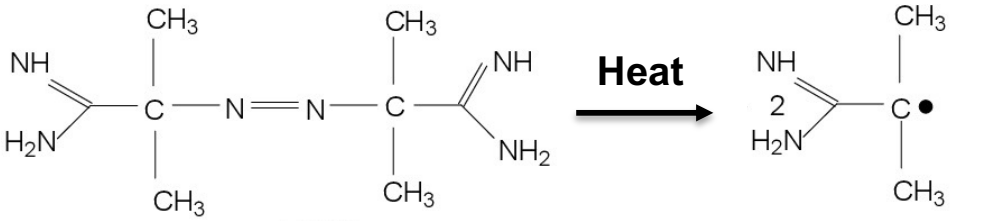

- AAPH is a water-soluble azo compound that can decompose and generate carbon-centered free radicals
- The decomposition rate of AAPH increases dramatically with temperature when the temperature is higher than 40°C.
- The carbon-centered free radicals generated by AAPH are highly reactive and can damage lipids, proteins, DNA, and other biomolecules

IONCs of 40 nm (with 6 nm primary MNPs) were coated with poly(AA-co-AMPS)-PEG for water-solubility and loading of AAPH to the carboxyl group of the coating

Zhang *et al,* ACS Nano, 2022

Heat and free-radical generation

IONC-AAPN was under AMF (H = 9.35 kA/m and f = 320 kHz) for 1 hour

40 nm IONCs with 6 nm primary MNPs

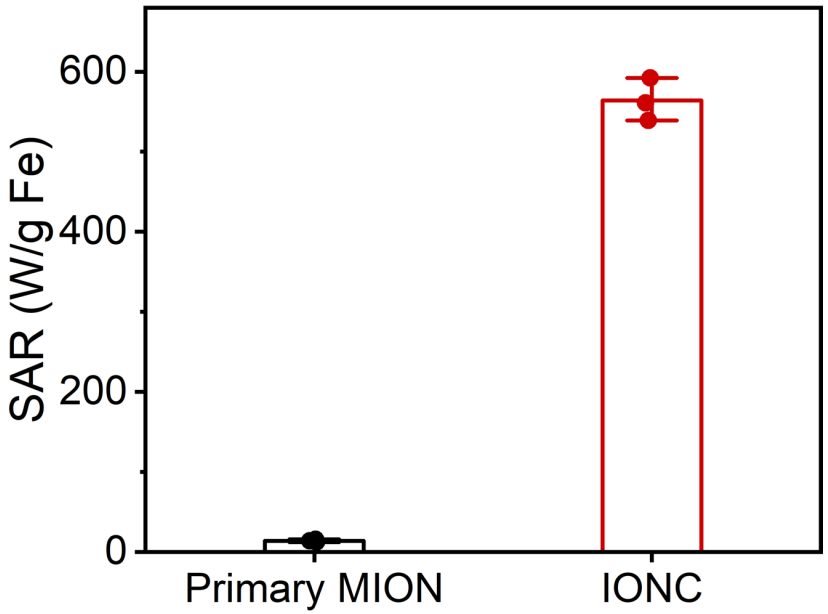

Free radical generation by IONC-AAPH

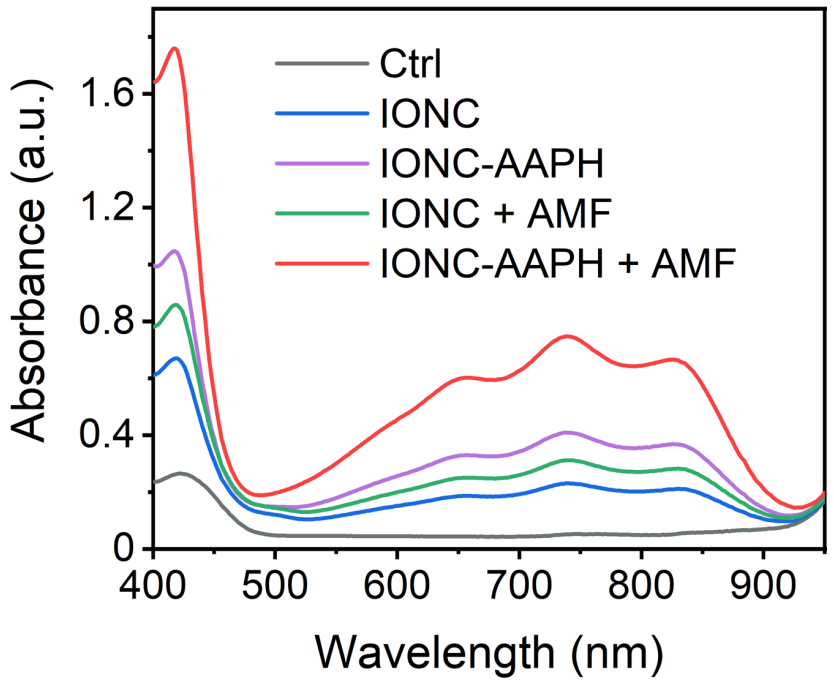

- ABTS reacts with the free radicals generated by AAPH and forms $ABTS^{+*}$
- $ABTS^{+*}$ has characteristic absorbance between 400-900 nm
- The absorbance peak is at 734 nm

Zhang *et al,* ACS Nano, 2022

Free radical generation and cell-killing by IONC-AAPH in cell culture

Flow cytometry analysis of free radicals in MC-38 cells via fluorescence from DCF

H_2DCFDA, a cell-permeant compound, was delivered to cells. Upon oxidation by free radicals, the non-fluorescent H_2DCFDA is converted to highly fluorescent DCF

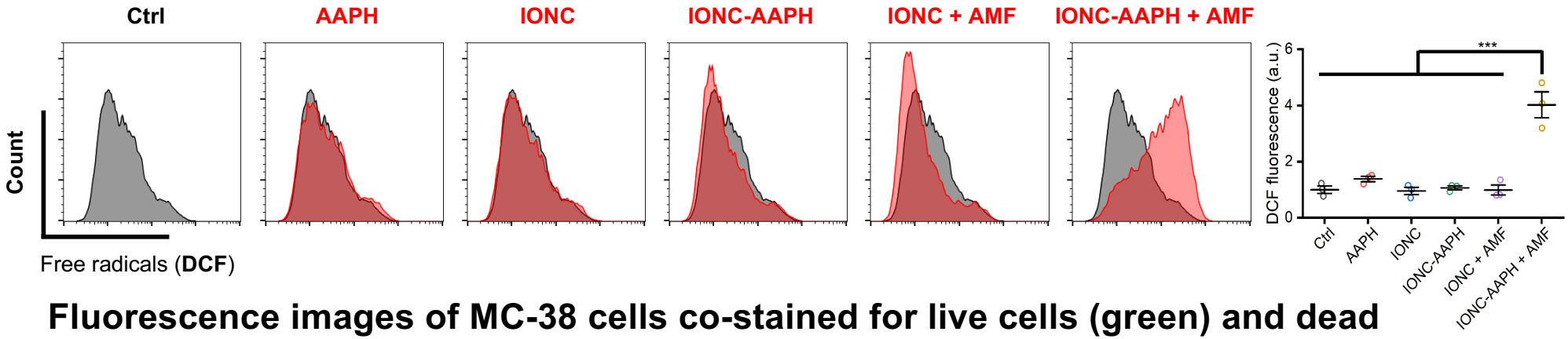

Fluorescence images of MC-38 cells co-stained for live cells (green) and dead cells (red) with different treatments under normoxic and hypoxic conditions

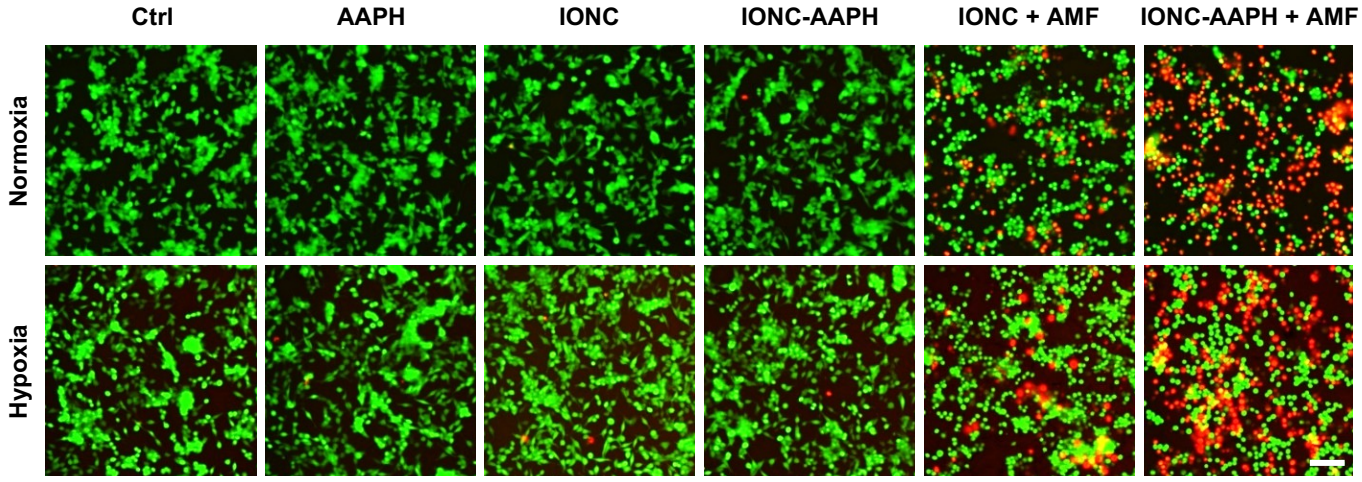

Cells were incubated with IONC-AAPH for 1 h for deliver followed by exposure to AMF for 1 h

Zhang *et al,* ACS Nano, 2022

Mechanisms of IONC-AAPH mediated cell killing

γ-H2AX foci assay to quantify DNA damage due to IONC-AAPH

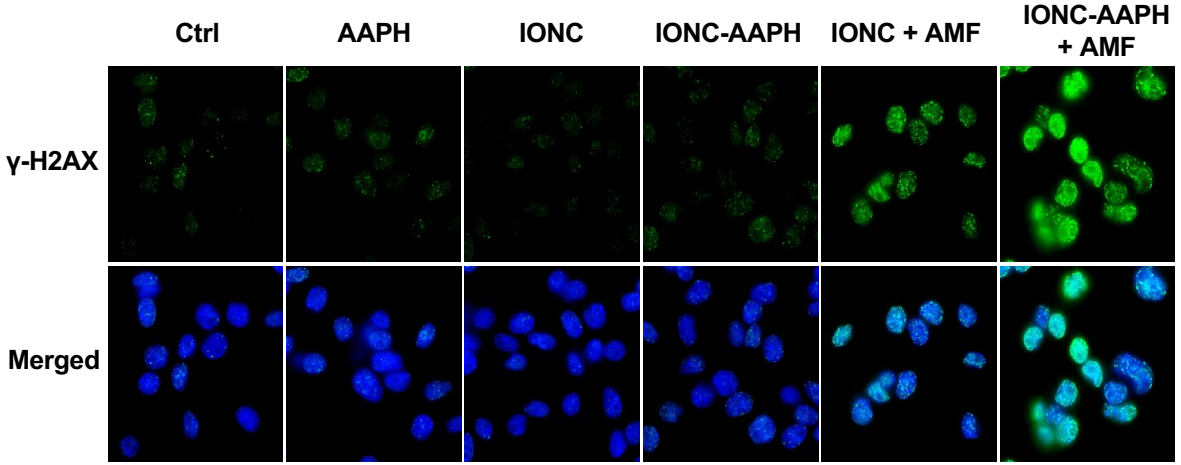

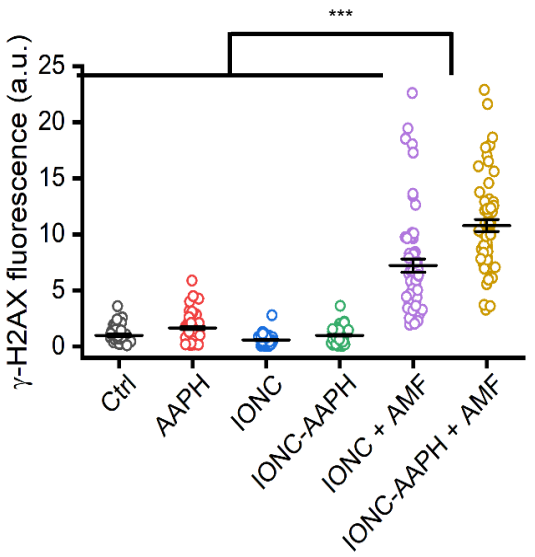

F-actin structure changes in MC-38 cells due to IONC-AAPH

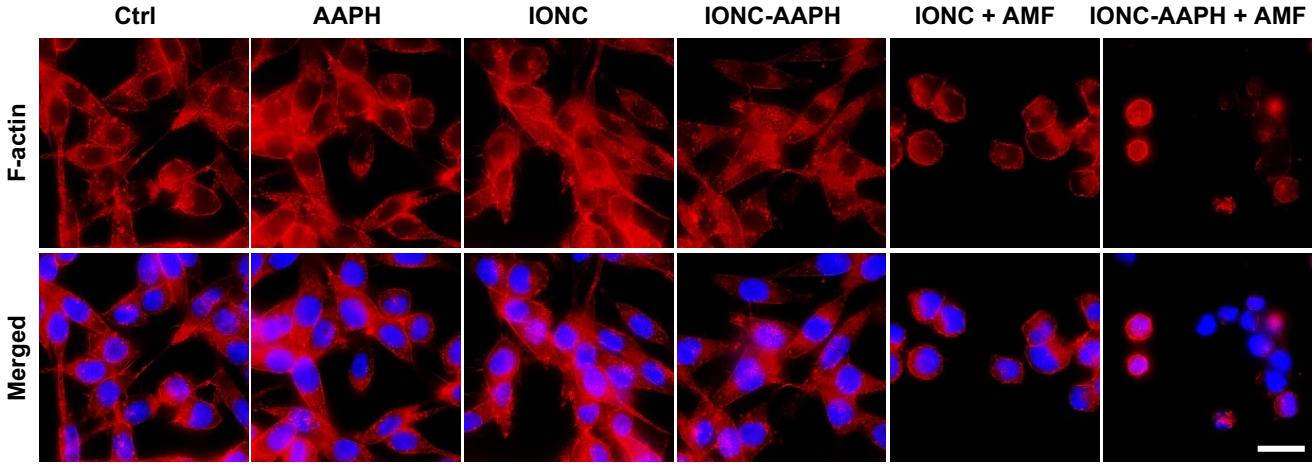

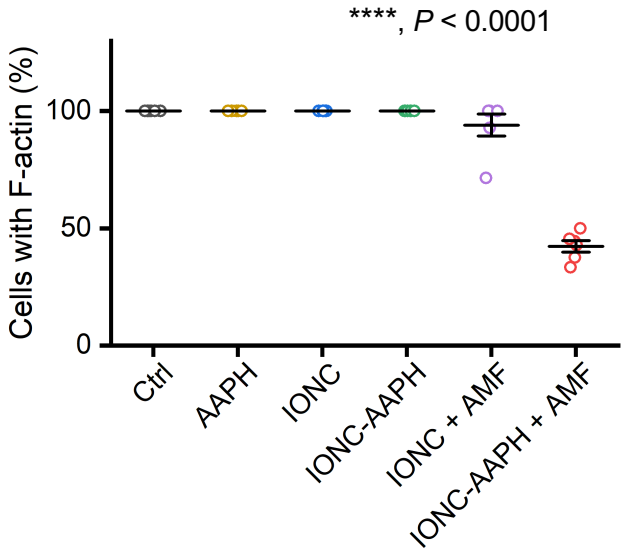

Zhang *et al,* ACS Nano, 2022

Anti-tumor effect of IONC-AAPH *in vivo*

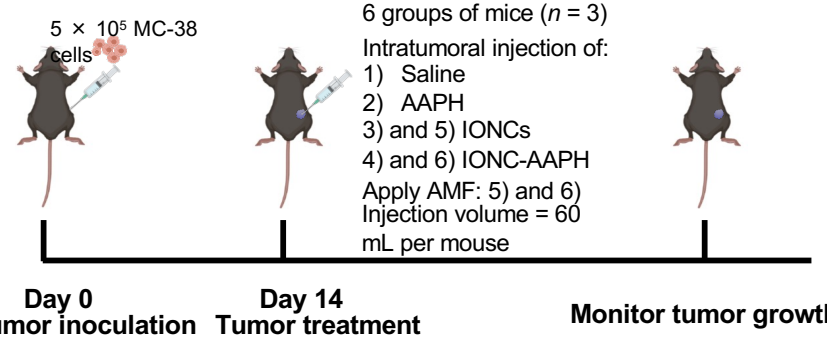

Mice were subjected to AMF (H = 9.35 kA/m and f = 320 kHz) for 80 min

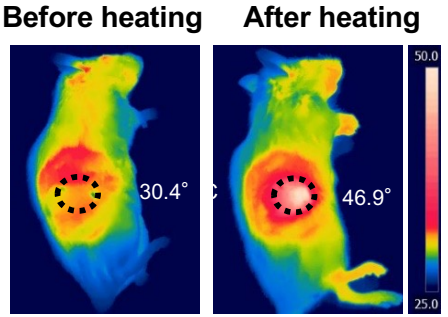

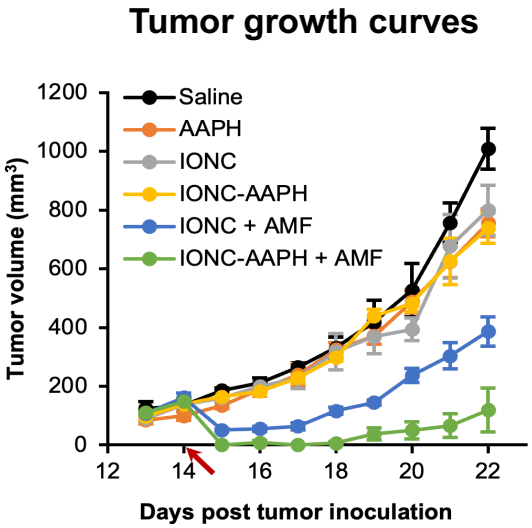

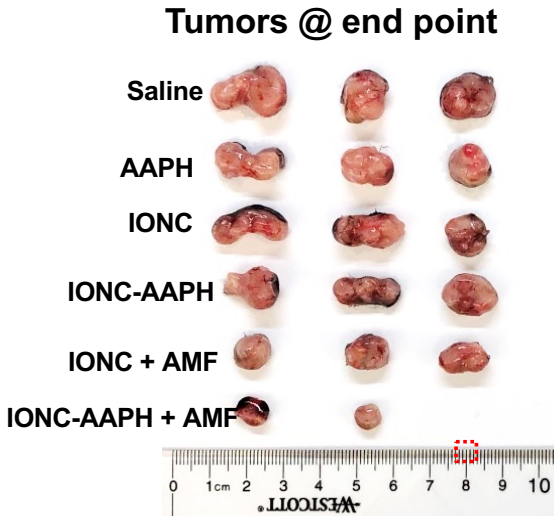

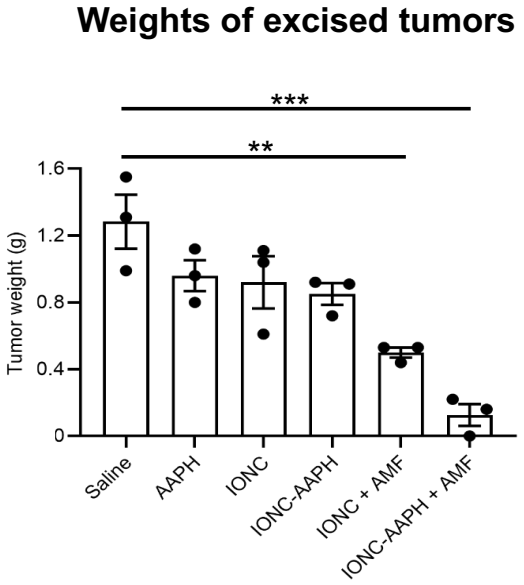

MC-38 is a colon cancer cell line

Zhang *et al,* ACS Nano, 2022

IONC-AAPH and ICB suppresses cancer metastasis

Metastasis is the predominant cause of cancer deaths (~80%) due to solid tumors, however anticancer drugs are not effective in treating metastatic cancer

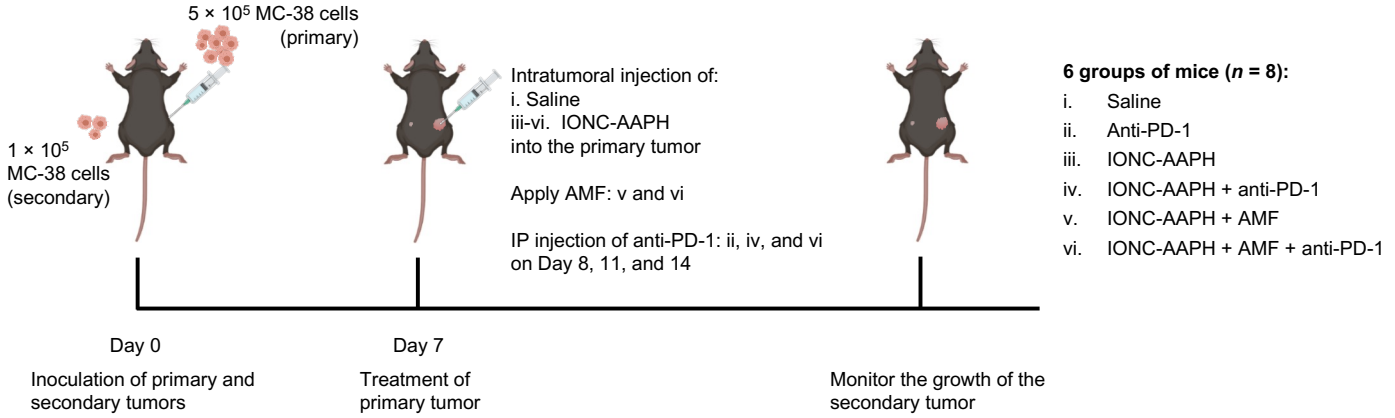

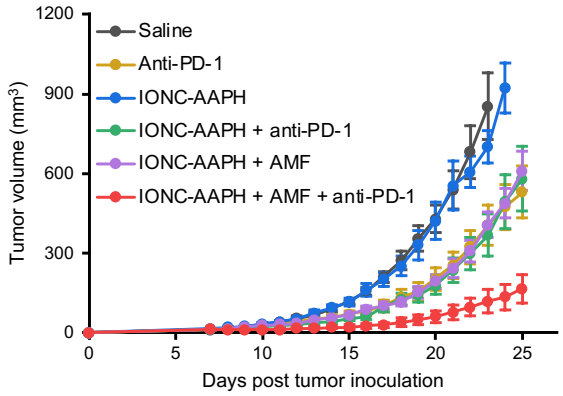

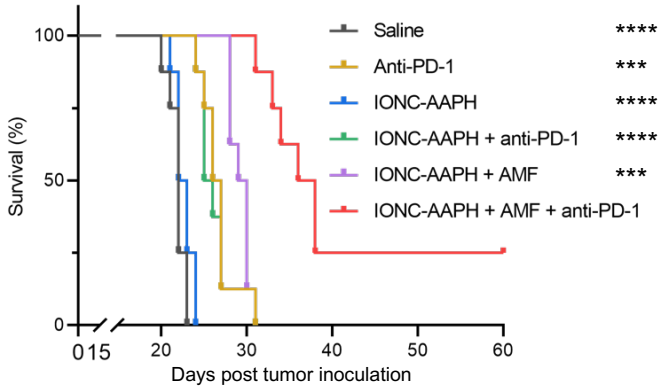

- The percentage of $CD3^+CD8^+$ T cells in the secondary tumors increased in the mice injected with IONC-AAPH
- The number of antigen-specific interferon-γ producing T cells was significantly higher in the mice treated with magneto-immunotherapy, 4.5-fold higher than that of control

Zhang *et al,* ACS Nano, 2022

Infiltrating CD8+ T Cells in Secondary Tumors

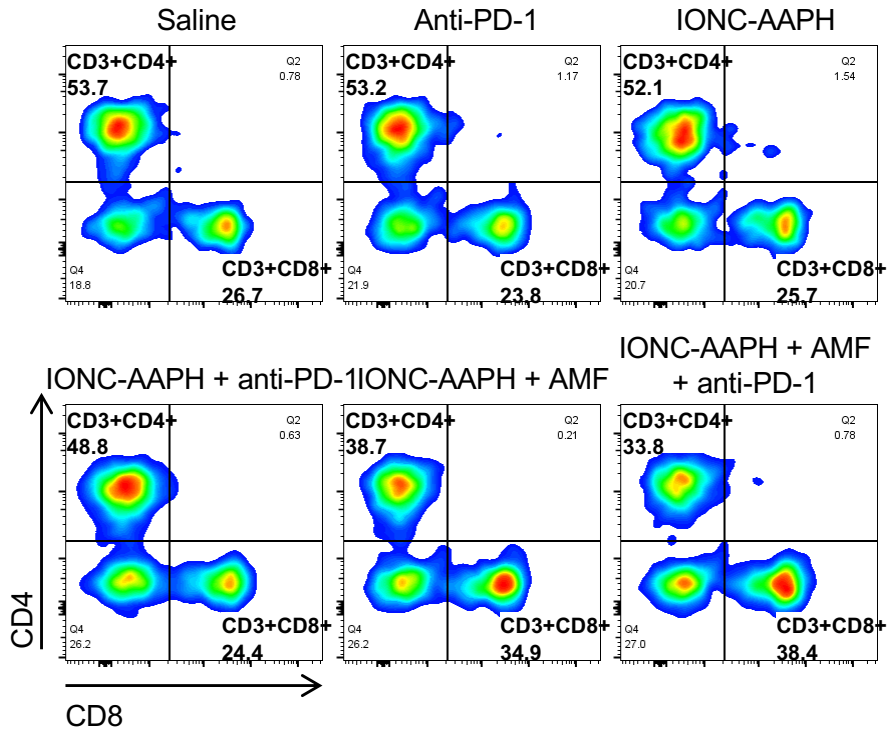

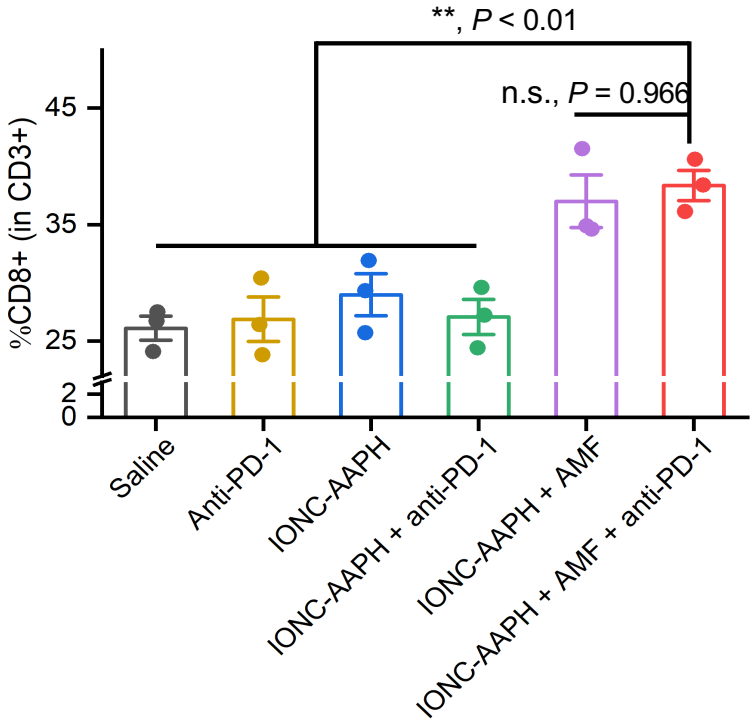

- 10 days after treating the primary tumor, cells in the secondary tumor without any treatment were harvested for flow cytometry analysis
- The percentage of $CD3^+CD8^+$ T cells in the secondary tumors increased by >2-fold in the mice injected with IONC-AAPH under AMF

Zhang *et al,* ACS Nano, 2022

Tumor antigen-specific T cells determined by ELISpot assay

Enzyme-linked immunospot assay

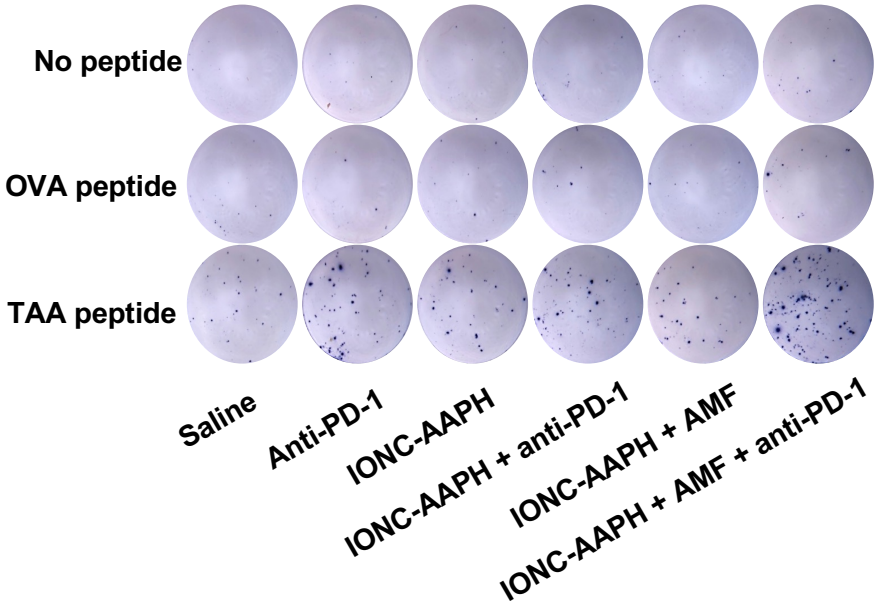

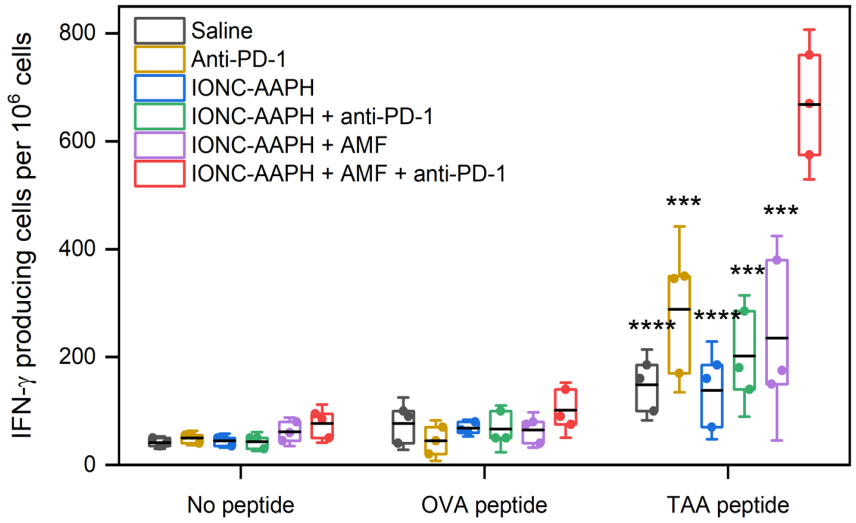

- The splenocytes were harvested and stimulated for 24 h with KSPWFTTL, a tumor-associated antigen (TAA) peptide. OVA: peptide SINFEKL
- In the mice treated with magneto-immunotherapy, the number of antigen-specific interferon-γ producing T cells was 4.5-fold higher than that of control

ACS Nano, Nov, 2022

Magneto-immunotherapy can suppress tumor recurrence

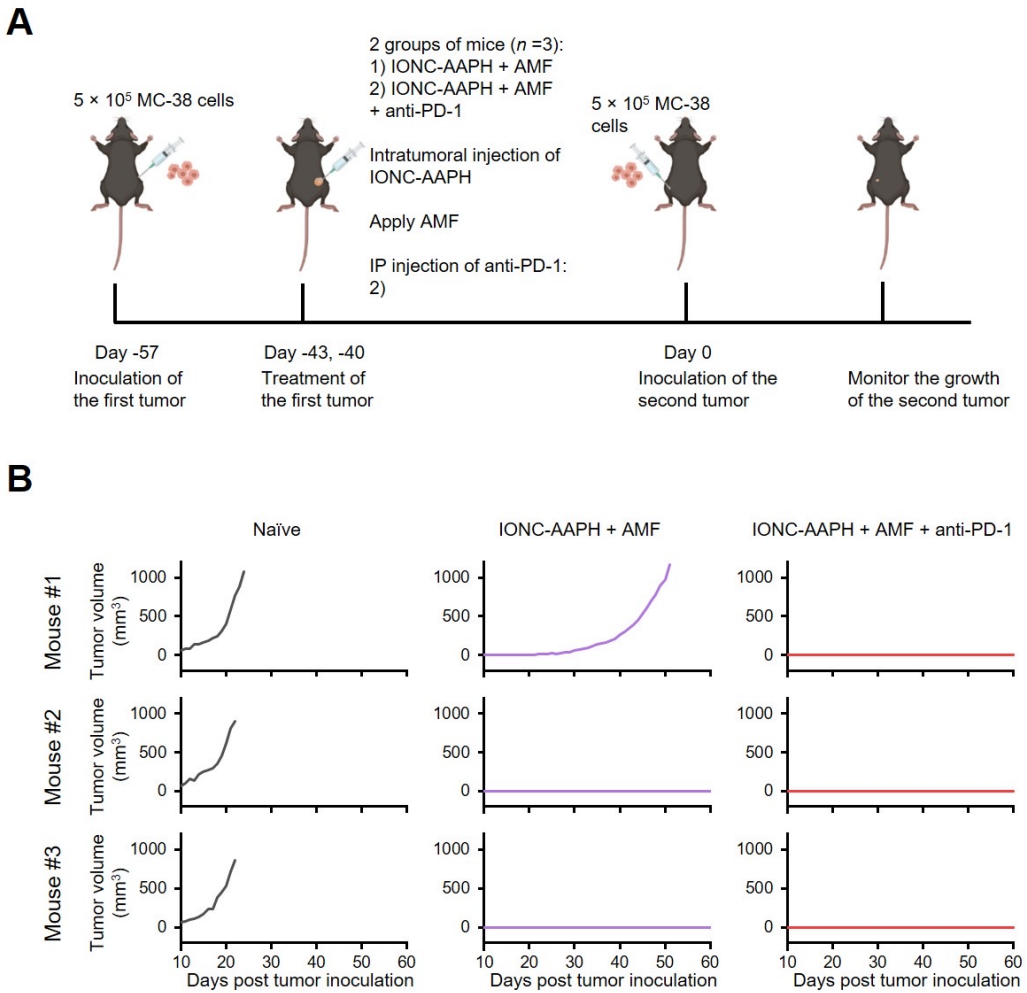

Nanocluster distribution 16 days post injection

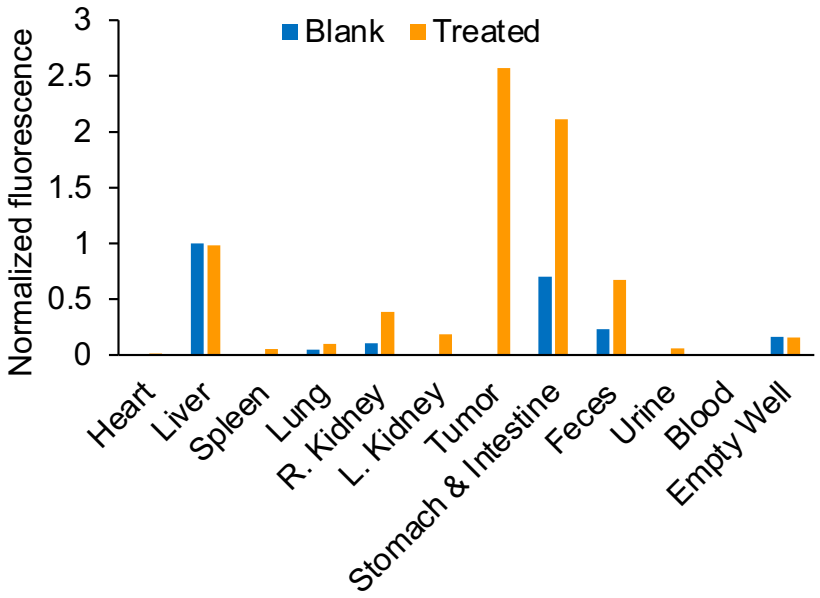

- True signals from tumor, digestive system and feces, background autofluorescence in liver
- We are now testing the approach for treating PDAC (pancreatic ductal adenocarcinoma)

Zhang *et al,* ACS Nano, 2022

Safety of IONC-AAPH in cancer therapy

H&E staining of major organs 24 h after treatment, showing no tissue damage due to IONC-AAPH

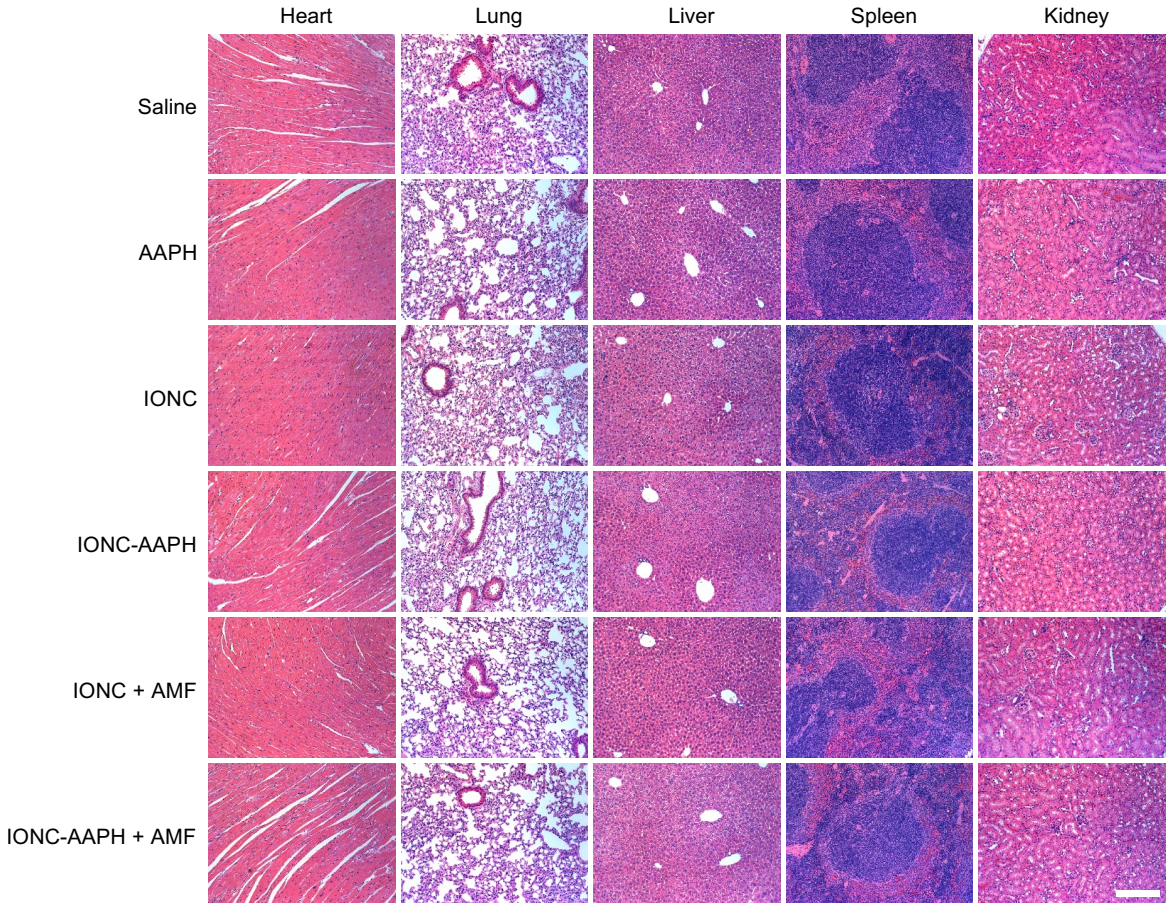

Evaluation of **liver function (**ALT, AST, & ALP in plasma) and **kidney function** (BUN in plasma) at end point

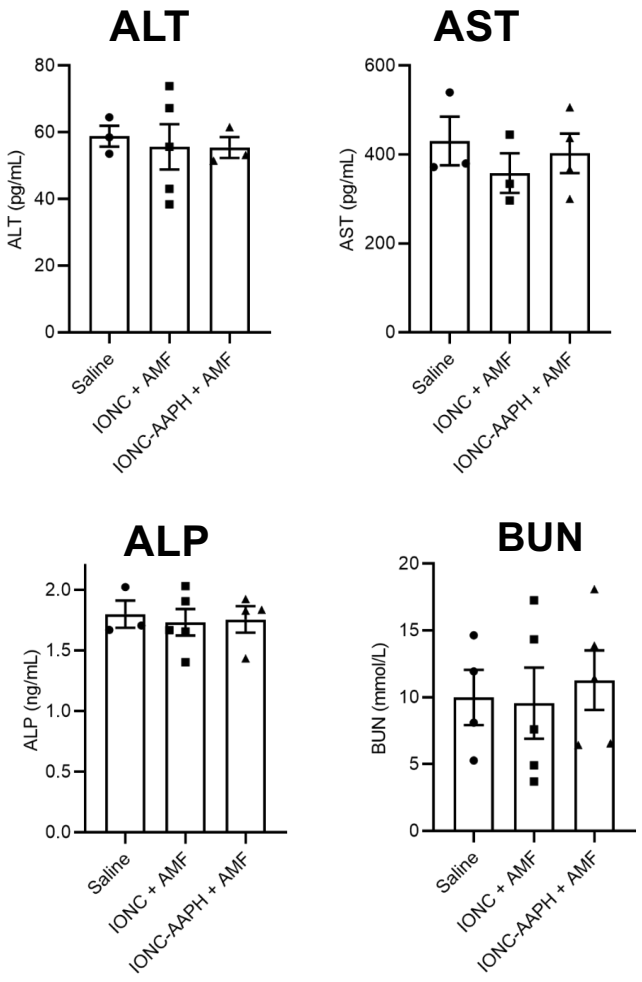

Zhang *et al,* ACS Nano, 2022

Companies Have Developed Large Systems for Applying Alternating Magnetic Fields

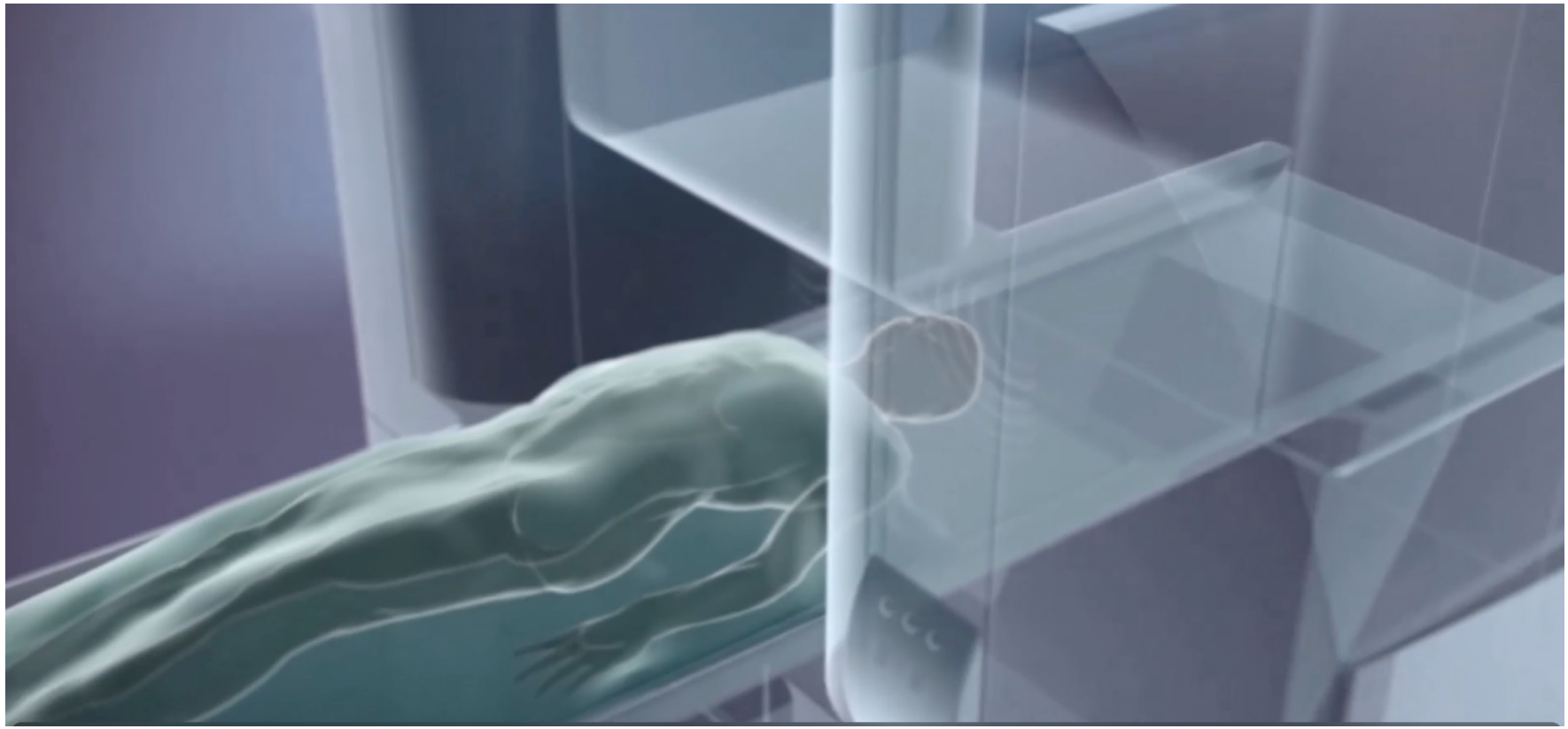

MagForce AG, a publicly traded company in Berlin, Germany

https://www.magforce.com/en/home/our_therapy/

Genome Editing – To Precisely Modify A Genome

Engineered nuclease cuts DNA at a user-defined site

DNA Repair Pathways

Error-prone repair

Non-homologous end joining
(NHEJ)

- Gene disruption
- Targeted DNA deletion

Programmed repair

Homology-directed repair
(HDR)

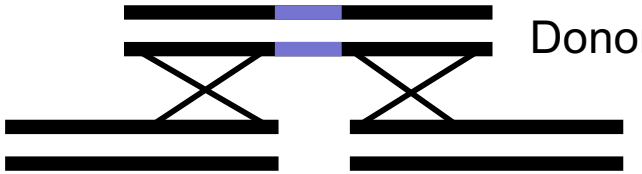

- Gene editing / correction
- Targeted gene insertion/tagging

Ex Vivo versus *In Vivo* Therapeutic Genome Editing

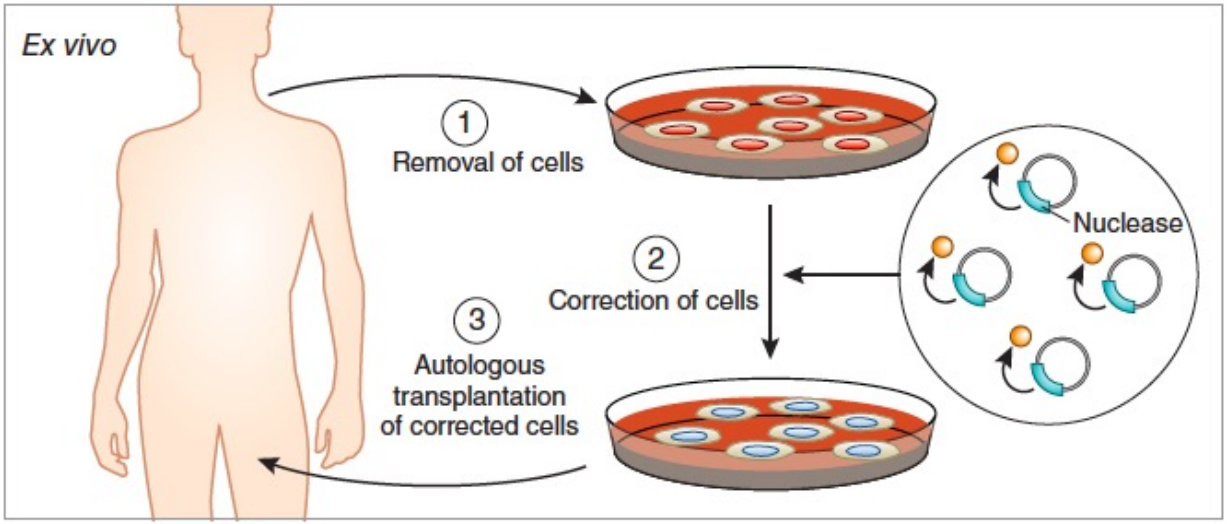

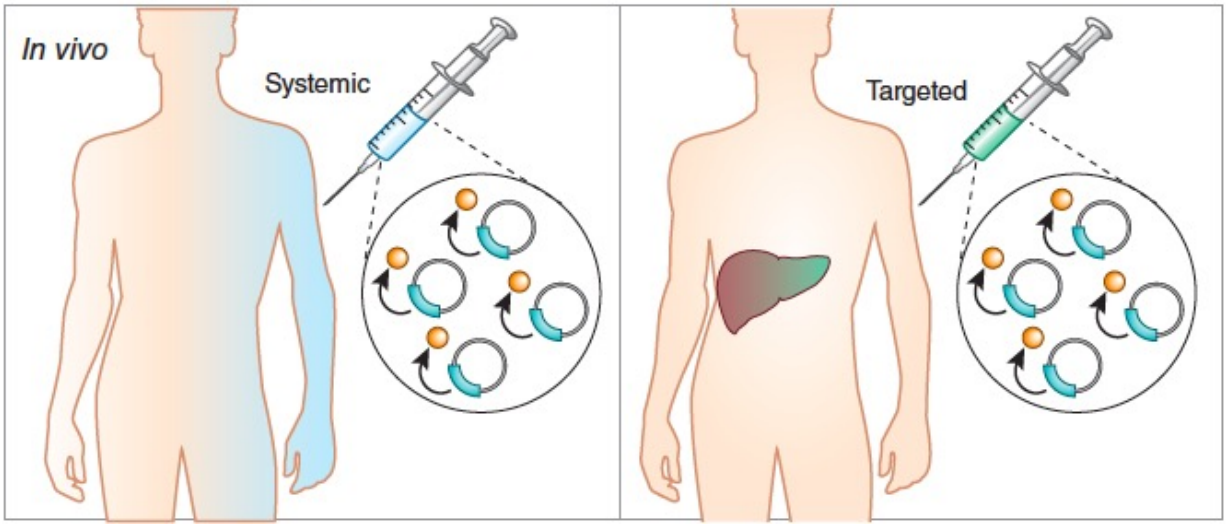

- ***Ex Vivo* Genome Editing**: delivery is easier but target cells must be capable of surviving outside the body and homing back to target tissues after transplantation

- ***In Vivo* Genome Editing**: With *in vivo* systemic delivery, high efficiency and tissue specificity is a challenge, and local injection might not give the desired distribution

Cox *et al.*, *Nature Medicine* (2015)

Sickle Cell Disease (SCD)

Cause: A-T mutation in the beta-globin gene. It occurs when a person inherits two mutant copies of the beta-globin gene, one from each parent


Sickle Cell Anemia

Statistics:

- SCD affects over 20 million people worldwide, including ~100,000 in the U.S., resulting in ~120,000 deaths every year

Treatment:

- Bone-marrow transplantation is the only cure
- Only ~15% of SCD patients could have a matching donor
- No cure for the majority of patients

Platt *et al.*, *N Engl J Med* (1994)

http://www.cdc.gov/ncbddd/sicklecell/data.html

Genome Editing Approaches for Curing SCD

- **Disrupting *BCL11A* enhancer in SCD HSPCs**[1,2]
- **Correcting *HBB* sickle mutation in SCD HSPCs**
  - Using AAV6 donor[3,4,5]
  - Using ssODN donor[6,7]
- **Base editing of SCD HSPCs**
  - Base editing of *BCL11A* enhancer[8]
  - Conversion of sickle allele in HBB (HBB^S) to Makassar β-globin (HBB^G)[9]

[1]Wu *et al, Nat Med*. 25:776-783 (2019); [2]Frangoul *et al*, *N Engl J Med*. 384:252-260 (2021); [3]DeWitt *et al*, *Sci Transl Med*. 8:360ra134 (2016); [4]Lattanzi *et al, Sci Transl Med*. 13:eabf2444 (2021); [5]Dever *et al*, *Nature* 539:384-389 (2016); Humbert *et al*, *Sci Transl Med*. 11:eaaw3768 (2019); [6]Park et al, *NAR*. 47:7955-7972 (2019); [7]Zeng *et al*, *Nat Med* 26:535-541 (2020); [8]Newby *et al*, *Nature* 595:295-302 (2021)

Gene Correction for Treating SCD

Approach: Use CRISPR/Cas9 to generate a DSB near the mutation site, activate homology directed repair, correct the A-T mutation using donor DNA template

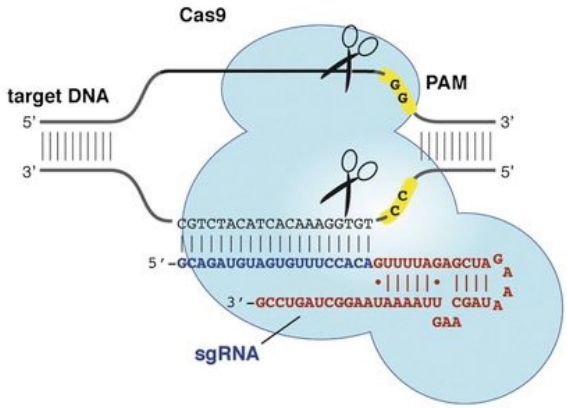

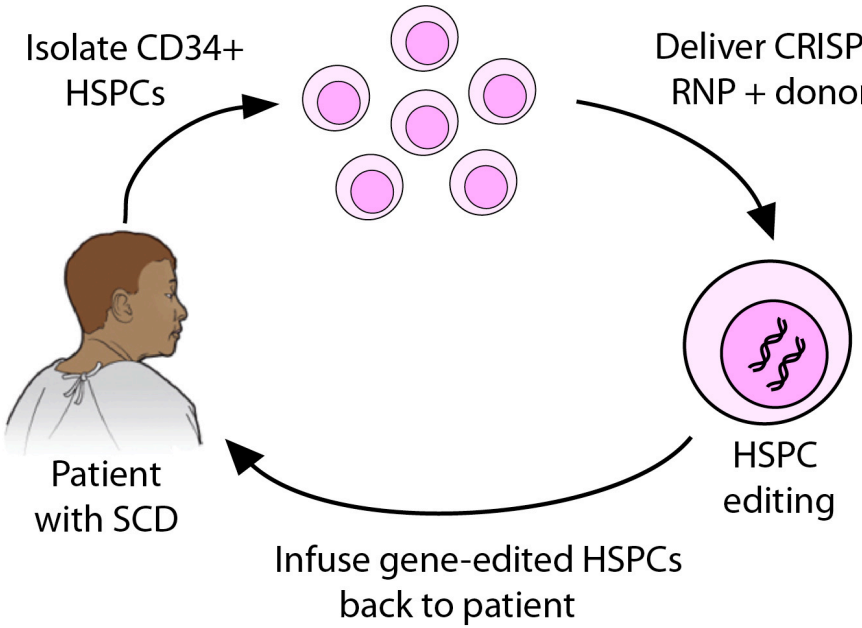

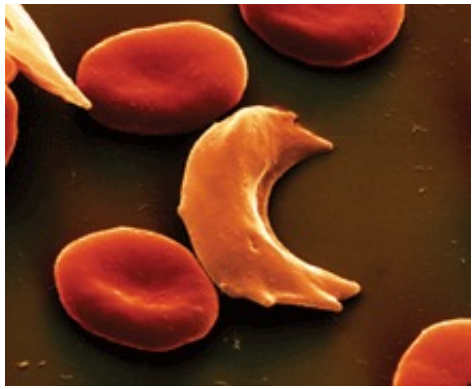

- Isolate hematopoietic stem and progenitor cells (HSPCs) from a SCD patient
- Damage the remaining HSCs in the patient using radiation or chemotherapy
- Deliver CRISPR/Cas9 and wild-type donor template into HSPCs for gene correction
- Deliver back the gene-edited HSPCs to the patient, produce normal red blood cells to replace sickle cells
- A few percent of gene-corrected HSCs can re-generate the who blood system

HBB Gene-editing to Cure SCD

- We have systematically optimized CRISPR gRNA and single-stranded DNA donor template (ssODN) designs
- Edited SCD CD34^{+} HSPCs by delivering Cas9/gRNA ribonucleoprotein (RNP) complex and corrective ssODN template using electroporation
- Achieved high rates of gene correction (HDR) in HSPCs from patients with SCD, and a high level of HbF induction by Cas9 cutting only
- Performed a genome-wide unbiased off-target analysis and significantly reduced off-target effects
- Demonstrated a good level of engraftment of gent-edited SCD HSPCs in immunodefficient NSG mice

Park *et al,* NAR, 2019

Gene Correction of CD34+ HSPCs from 5 SCD Patients

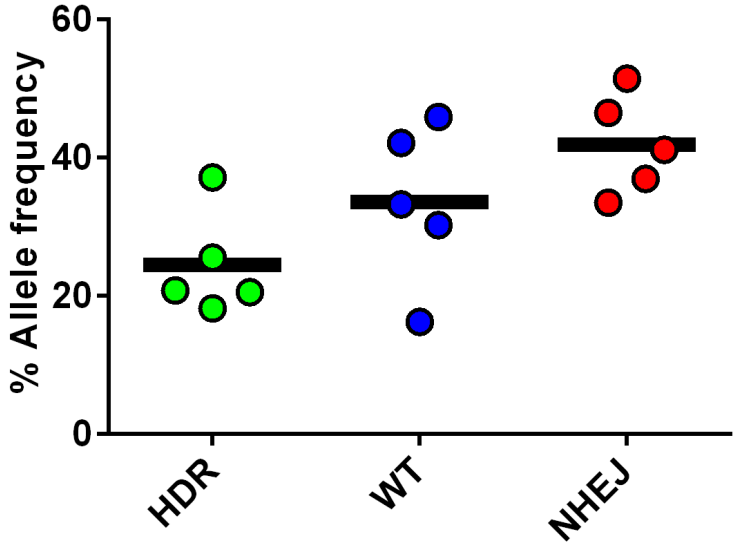

The results of HBB gene correction in CD34+ HSPCs from five SCD patients using gRNA/Cas9 RNP and SCDct5-wt ssODN.

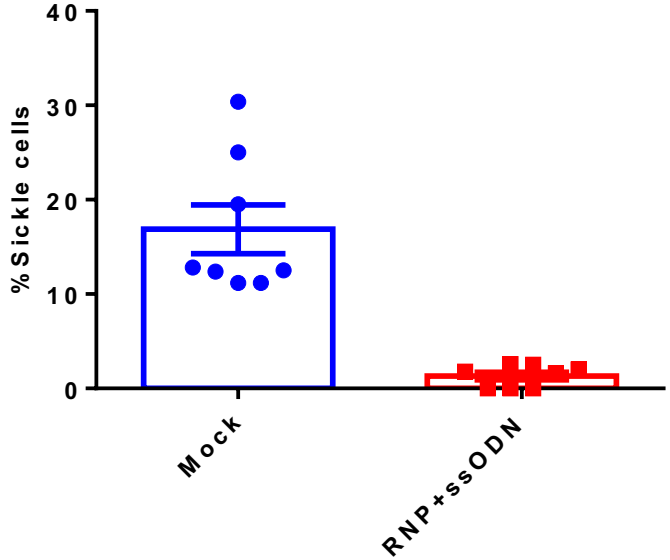

SCD HSPCs after gene editing were differentiated for 3 weeks. At day 21, sickled cells were counted and the percentage of sickled cells quantified

Park *et al,* NAR, 2019

Gene Correction of SCD CD34+ HSPCs Induced a High Level of Normal Beta-globin

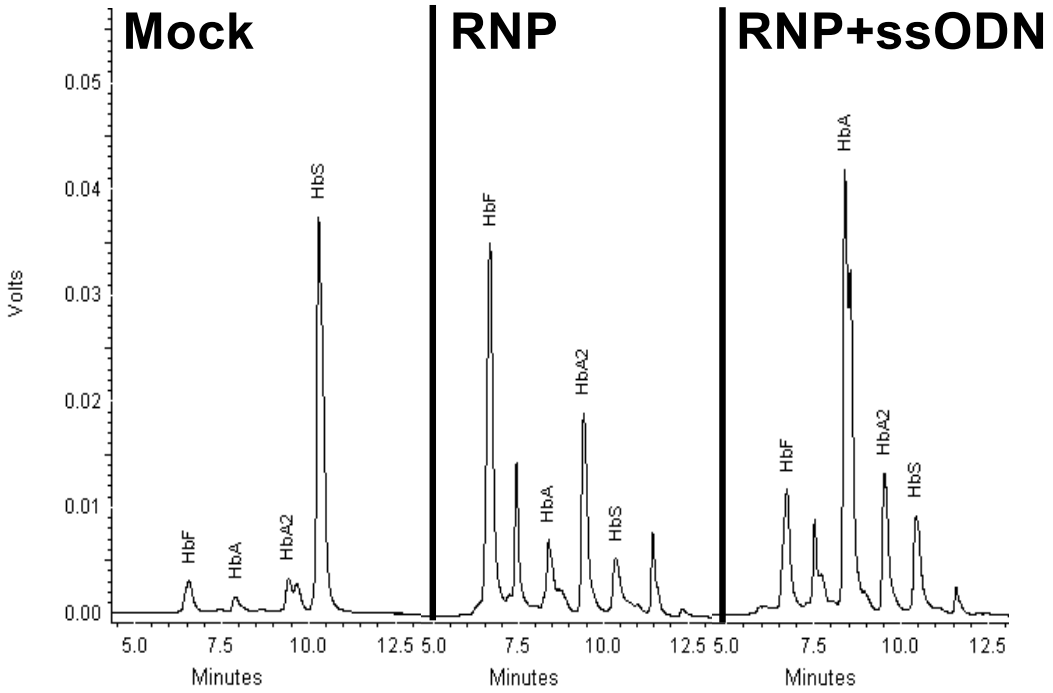

HPLC trace showing hemoglobin production after 21 days of differentiation of gene-edited SCD HSPCs

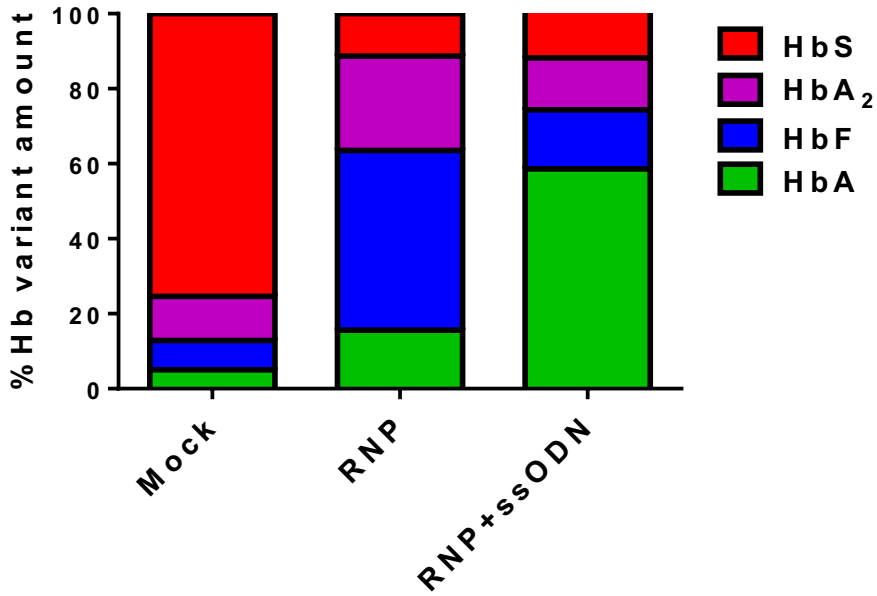

Delivery of gRNA/Cas9 RNP only into SCD HSPCs induced a high level of HbF expression

Park *et al,* NAR, 2019

Engraftment studies for IND application

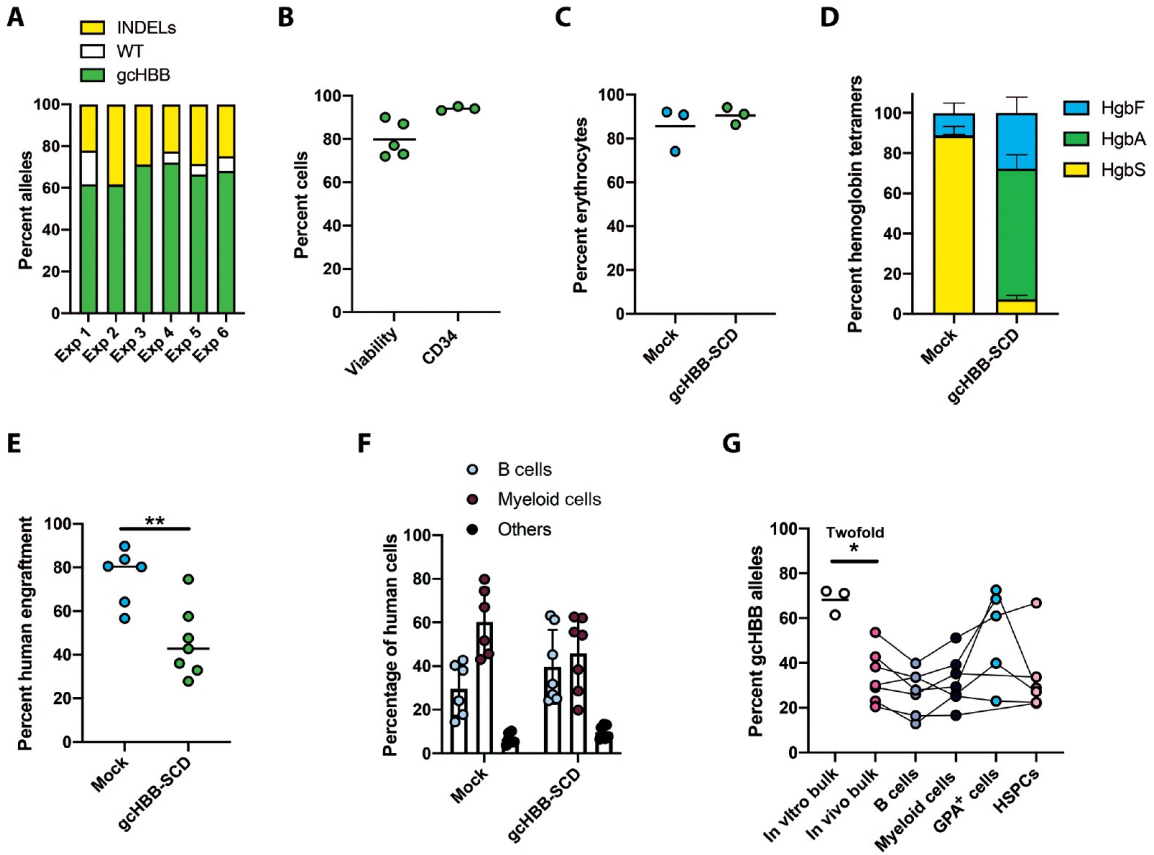

2 clinical trials using R-02 gRNA

- **GPH101**: Gene Correction in autologous CD34+ hematopoietic stem cells (HbS to HbA) to treat severe sickle cell disease (Matt Porteus and Graphite Bio)

- **CRISPR_SCD001**: Transplantation of CRISPR modified hematopoietic progenitor stem cells in patients with severe sickle cell disease (Mark Walters)

- Up to 60% HBB allelic correction in clinical-scale gcHBB-SCD manufacturing
- 20% gene correction with multilineage engraftment in NSG mice

Lattanzi *et al,* Sci Transl Med. 2021

Unintended Large Gene Modifications

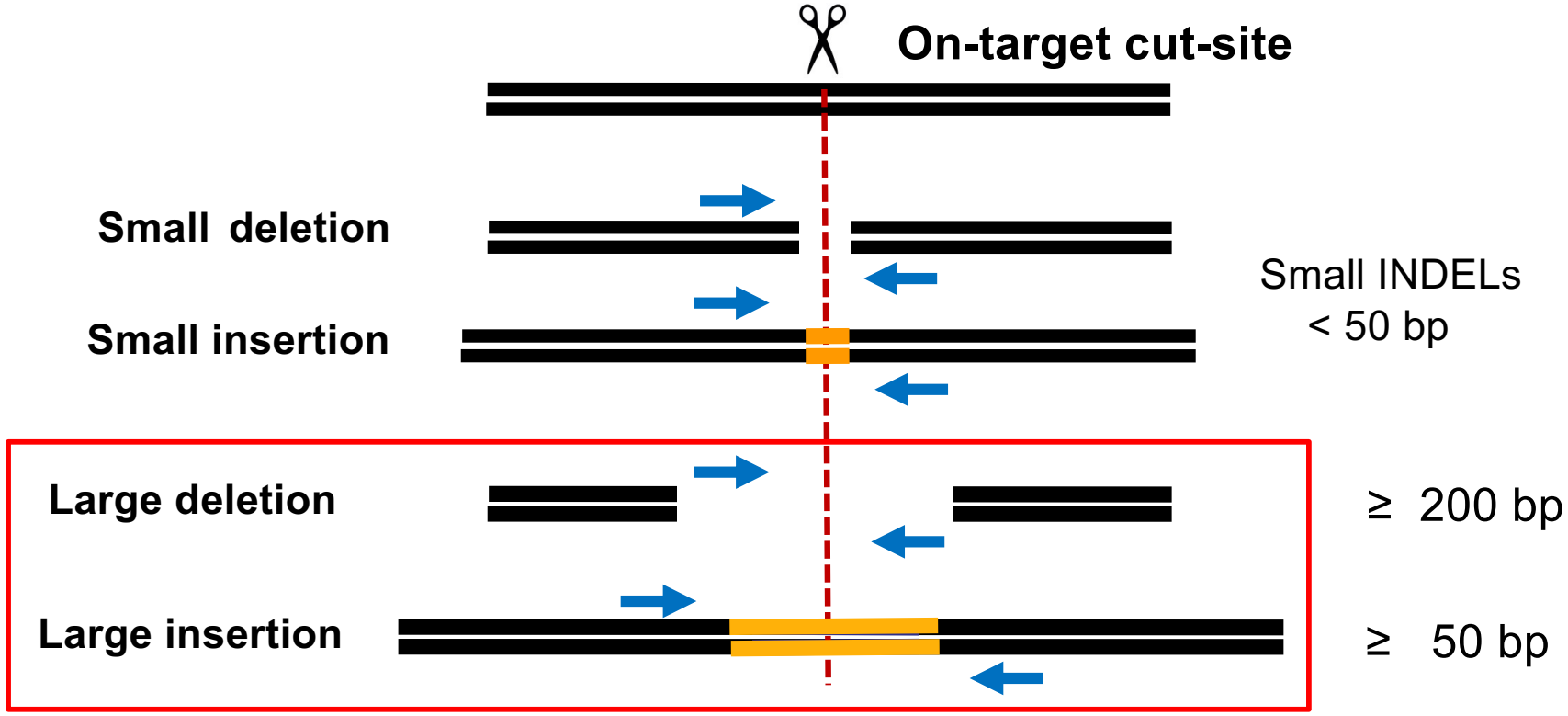

- On-target DNA DSBs could induce large deletions/insertions and complex local rearrangements, which may have pathogenic consequences
- Large deletions/insertions cannot be detected by short-range PCR and targeted deep sequencing due to loss of primer binding sites

Large Deletions/Insertions at the On-target Cut-site Quantified by SMRT-UMI

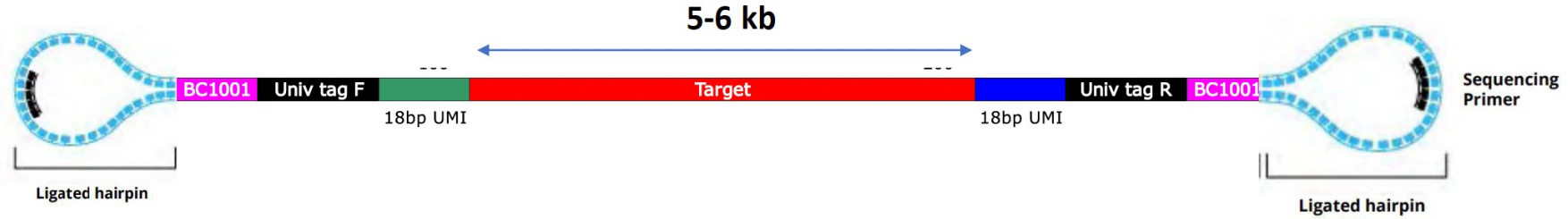

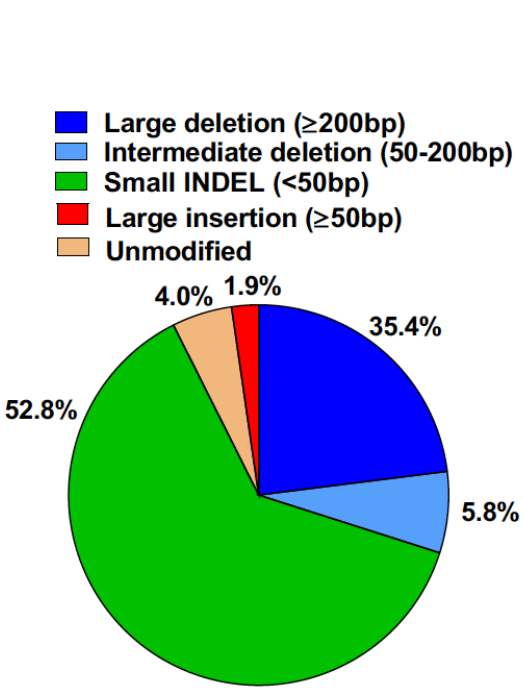

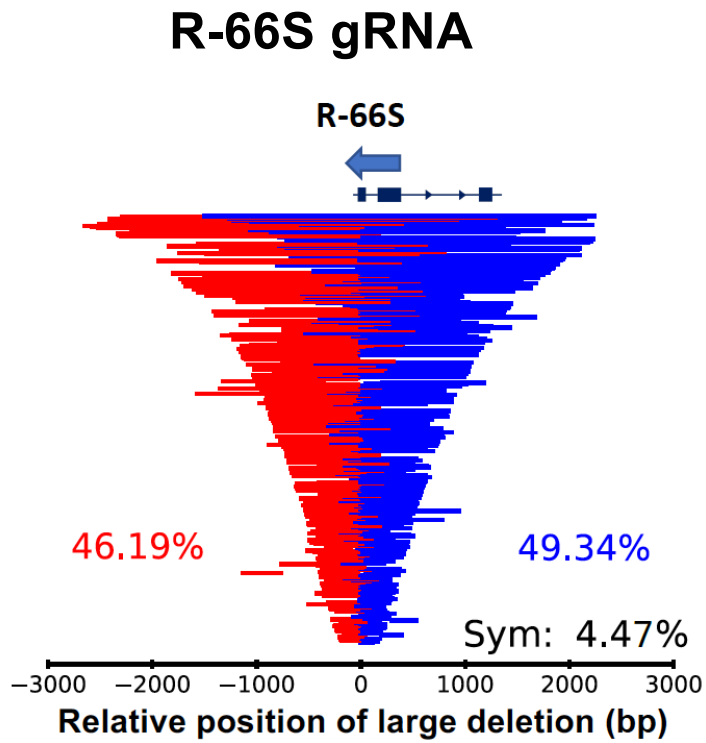

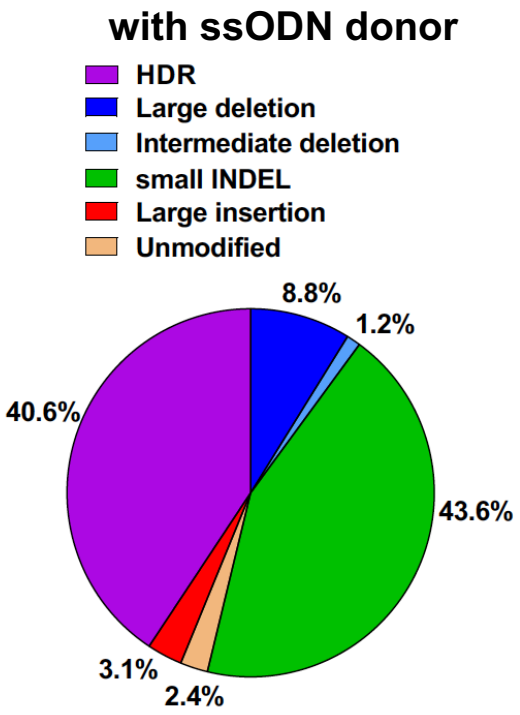

Park *et al,* Sci Adv 2022

UMI - Unique Molecular Identifier

Large Insertions at HBB On-target Cut-site due to R-66S RNP

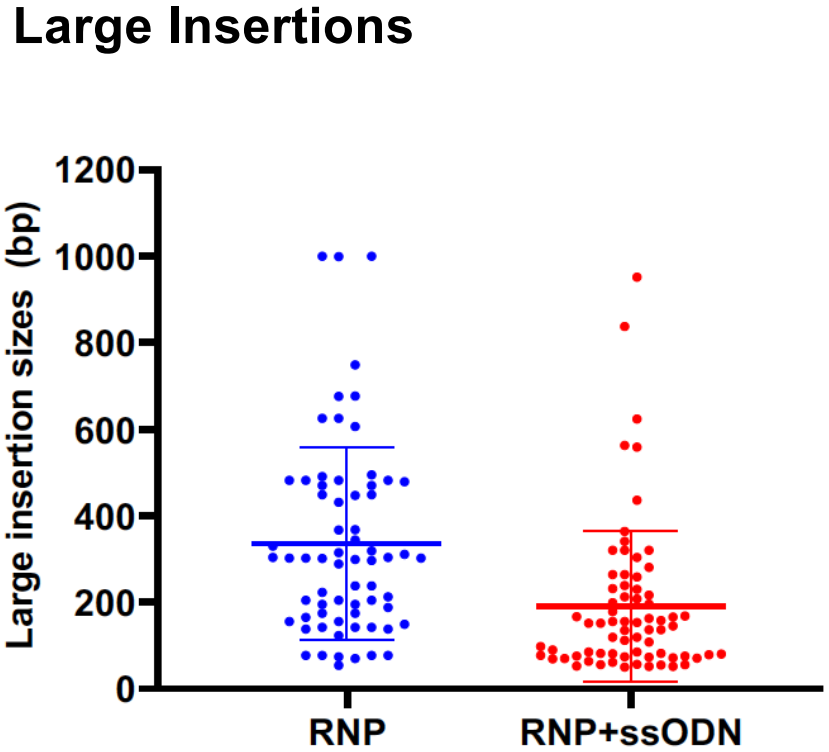

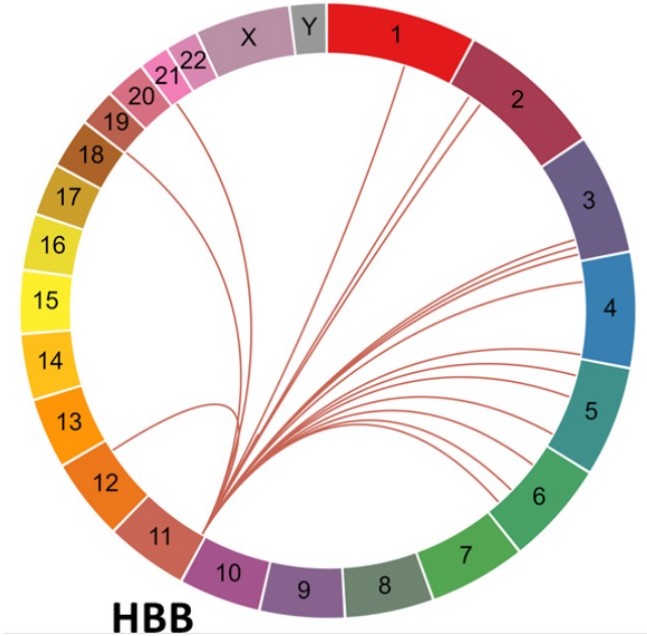

Park *et al,* Sci Adv 2022

Large Deletions and Insertions Occurred with Different gRNAs

gRNA	Target	Sequences
R-66S	HBB	GTAACGGCAGACTTCTCCACAGG
R-02	HBB	CTTGCCCCACAGGGCAGTAACGG
SD-02	HBG	CTTGTCAAGGCTATTGGTCAAGG
BCL11A	BCL11A	CTAACAGTTGCTTTTATCACAGG

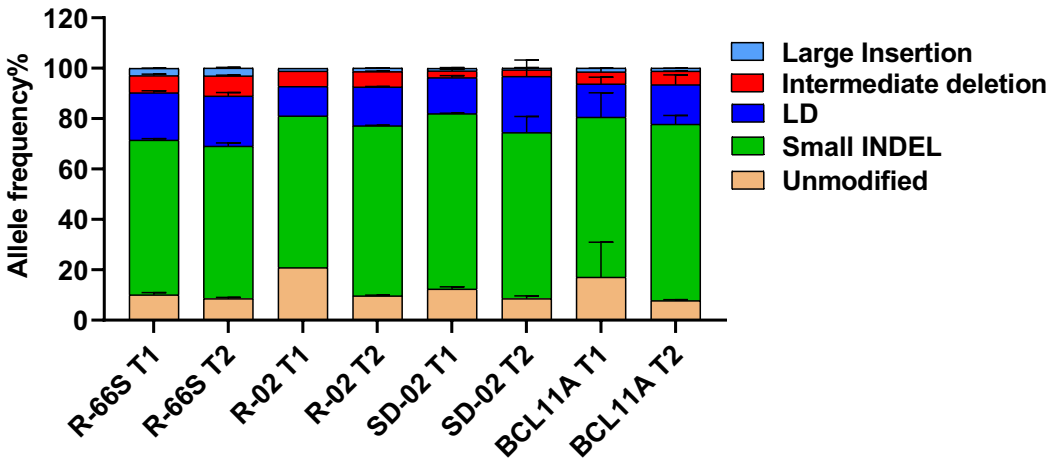

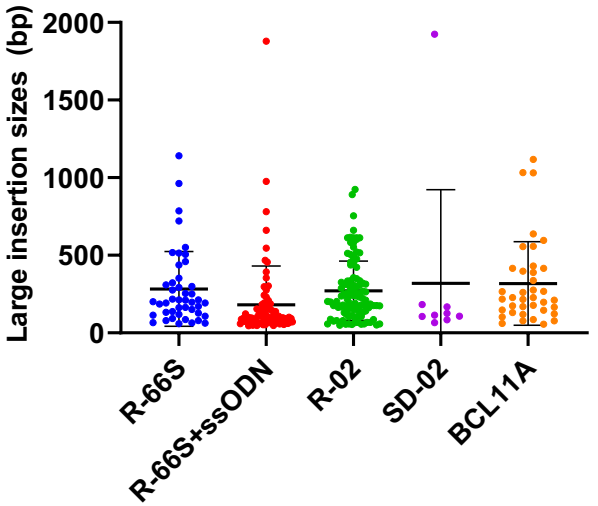

Park *et al*, Sci Adv 2022

Unintended Large Gene Modifications

- What is the mechanism that causes large deletions with high frequencies?
- What are the biological consequences of large deletions and insertions?
- How to reduce/eliminate large deletions and insertions?

In Vivo Gene Editing for Curing Diseases

- *Ex vivo* gene editing for curing SCD would not be feasible for patients in resource-poor regions, since it requires mobilization and isolation of HSCs from the patient for editing, chemo/radiation to damage remaining HSCs, and infusion of gene-edited HSCs to the patient. The estimated cost is ~$2 million per patient.

- *In vivo* gene editing for curing human diseases has significant challenges, including the need to achieve high editing rate *in vivo*, and the potential off-target organ/tissue editing.

- *In vivo* delivery using viral vectors such as AAV may suffer from uncontrollable expression of the editing machinery, causing immune response and genotoxicity.

- There is a need to achieve spatial and temporal control of *in vivo* gene editing, to minimize off-target tissue editing and immune response.

Spatial Control of *in vivo* Genome Editing via Nanomagnets

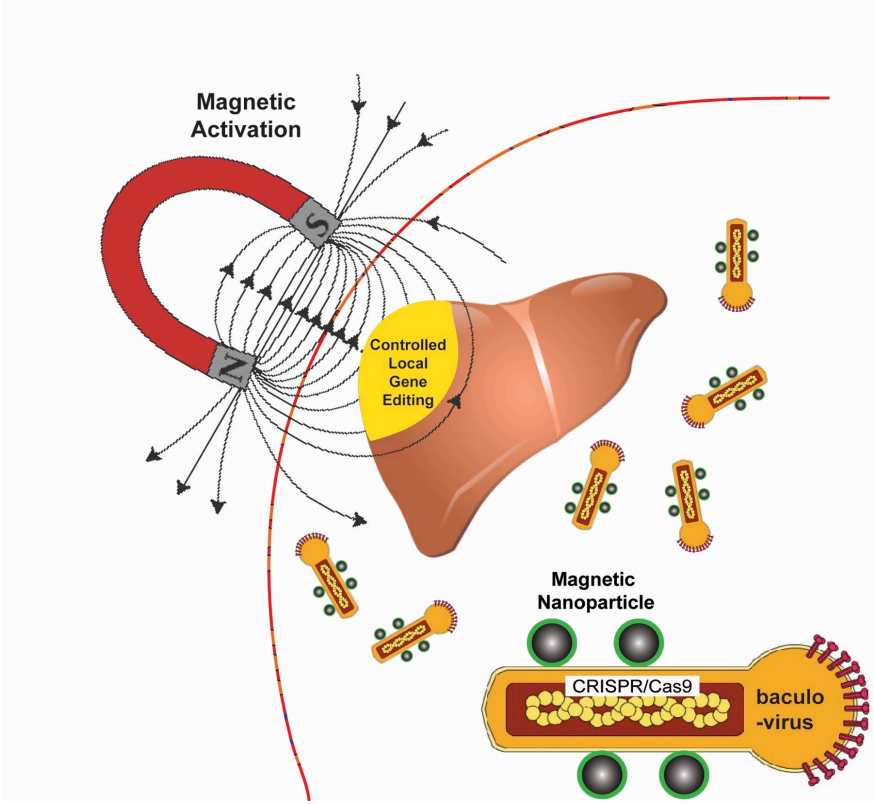

- During *in vivo* delivery, baculovirus (BV) vector is inactivated by the serum complement system
- When complexed with magnetic nanoparticles, BV can be activated locally with an applied magnetic field

BV-CRISPR expression vector

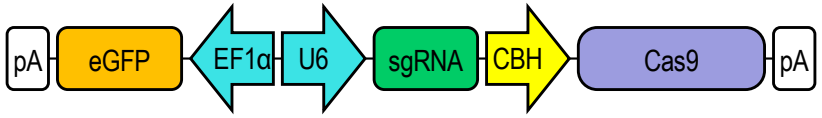

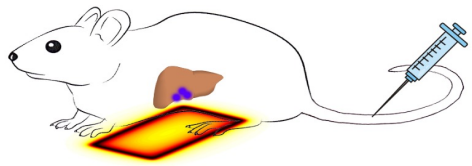

Mouse VEGFR2 gene editing *in vivo*

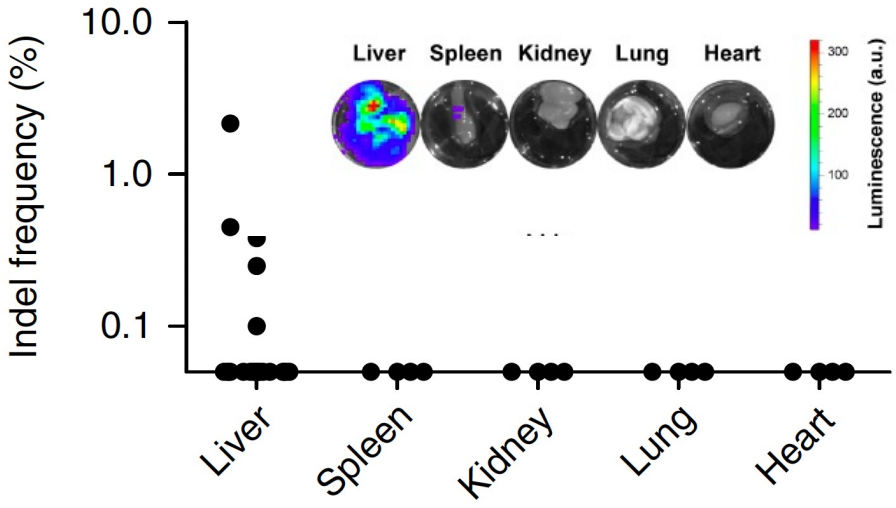

Zhu *et al.*, Nat BME, 2019

Summary

- We revealed the size-dependence of magnetic nanoparticle heating, demonstrating that the classic theory is incorrect for large MIONs (>15 nm)
- Magnetic iron oxide nanoclusters with AAPH have the potential to serve as a new nanotherapeutic agent to suppress cancer metastasis and recurrence
- We have developed gene editing based approaches for curing sickle cell disease and the pre-clinical results are very promising. Clinical trials are underway.

RICE

Bioengineering

Gordon Research Conference: Advanced Cell and Tissue Biomanufacturing

Advanced Cell and Tissue Biomanufacturing

Gordon Research Conference

Accelerating Cell and Tissue Manufacturing Technology Development and Innovation Through Convergence

June 25 - 30, 2023

Apply Now

Chairs

Kaiming Ye and Paul Carlyle. Goodwin

Vice Chairs

Gang Bao and James Hoying

Contact Chairs

Grand Summit Hotel at Sunday River

97 Summit Road

Newry, ME, United States

Venue and Travel Information

https://www.grc.org/advanced-cell-and-tissue-biomanufacturing-conference/2023/

RICE

Bioengineering

Acknowledgements

Bao Lab Members

Dr. Linlin Zhang
Dr. Qingbo Zhang
Dr. Sheng Tong
Dr. Julie Park
Mingming Cao
Dr. Ciaran Lee
Dr. Buhle Moyo
Dr. Haibao Zhu
Dr. Kevin Li
Dr. Yidan Pan
Dr. Cecile Karsenty
Lucas Brown
BY Yoo
Aidi Liu
Daniel Prasca-Chamorro
Ishika Khondaker

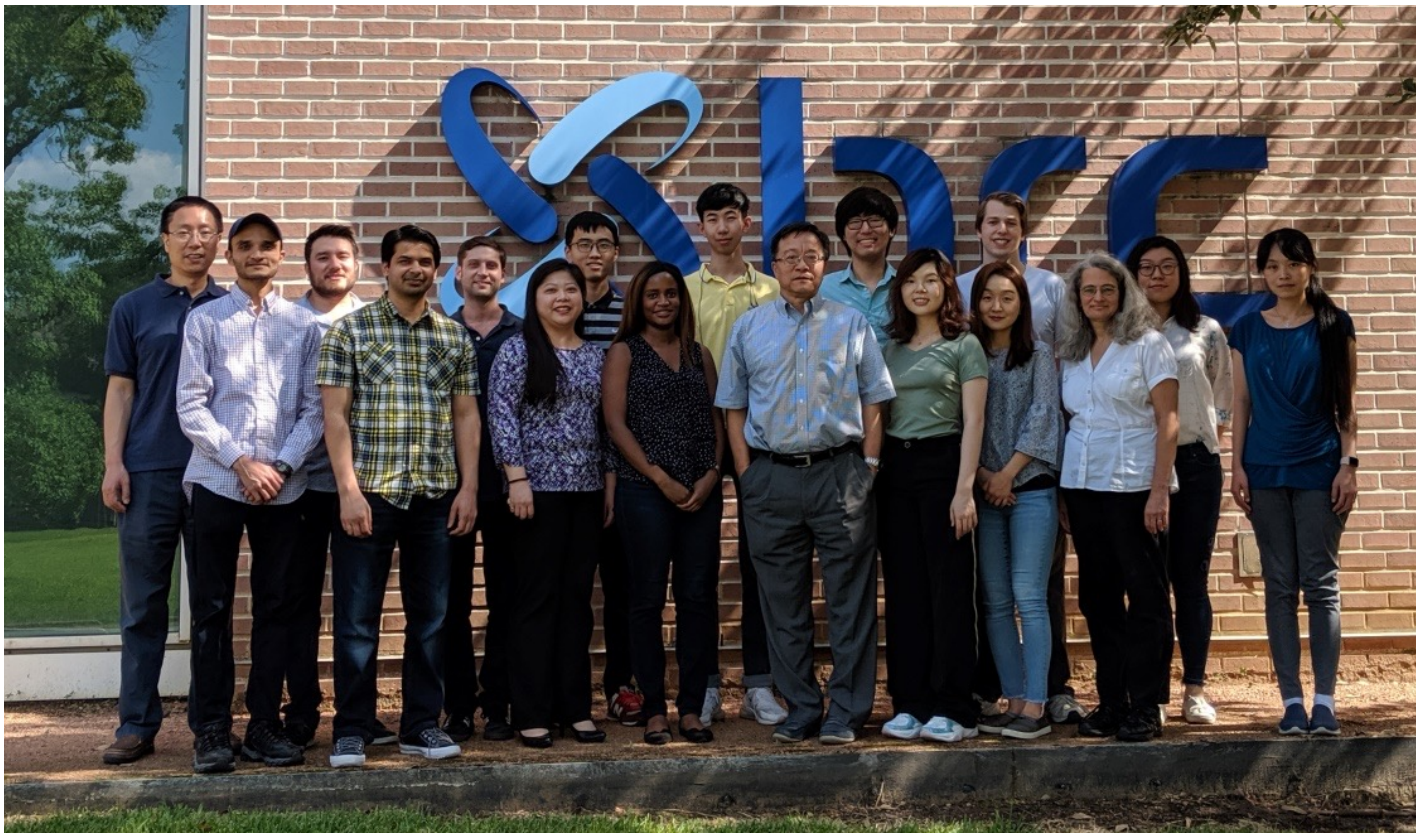

Adam Yaseen
Samira Hajebrahimi

Amy Tang
QK Pham

Collaborators on genome editing: Dr. Matt Porteus at Stanford
Dr. Vivien Sheehan at Emory